Benchmark Testing Plan

FHWA Project "Improving the Quality of Pavement Profiler Measurement"

FHWA Task Order "Evaluation of Potential Pavement Profile Reference Devices"

Developed by:

Steven M. Karamihas

University of Michigan Transportation Research Institute

September, 2009

Updated by:

Rohan W. Perera, Robert Orthmeyer, and Steven M. Karamihas

January, 2013

Table of Contents

Benchmark Testing Plan

This document presents the Benchmark Testing Plan for evaluating candidate reference profilers under the Federal Highway Administration (FHWA) project, "Improving the Quality of Pavement Profiler Measurement," (Contract No: DTFH61-07-C-00024) within Pooled Fund Study TPF-5(063). The procedures described in this document will be used in the 2012 evaluation of reference devices.

The technical approach to the testing plan follows the overall framework described in the Critical Profiler Accuracy Requirements (CPAR) report (Karamihas, 2005). In particular:

- Profile measurement accuracy, profile repeatability, and longitudinal distance measurement accuracy are the three primary measures of reference profiler performance.
- Reference profile measurement accuracy will be established through comparison to benchmark profile measurements on several test sections of diverse surface texture.
- A successful reference profiler must demonstrate repeatability and accuracy of IRI filtered profile and slope profile in three wavebands that collectively cover the waveband of interest.
- Profile repeatability and accuracy scores will be calculated using cross correlation.
- A successful reference profiler must demonstrate sufficient agreement with steel tape measurements of longitudinal distance.
- Along with the items above, reports of reference profiler performance shall include auxiliary information that may affect an agency's decision to purchase a device. These include speed of operation, ease of operation, pre-test calibration and system checks, and troubleshooting procedures.

Two technical aspects of the CPAR report will not be adopted:

- The designs offered for benchmark profile measurement in Chapter 7 will not be used. (See "Benchmark Profile Measurement" below.)
- The limits placed on gain error developed in Chapter 4 will not be enforced as requirements for profiler accuracy. Instead, spectral analyses such as gain, phase, and coherence plots will provide diagnostic information and verification of cross correlation results.

The CPAR report also specified several analysis settings, calculation methods, and threshold values. This Plan refines those selections based on research conducted since the report was completed. Many of the extensions to the CPAR report are the result of research within the FHWA Golden Footprint project, further analysis of the 2004 FHWA Profiler Round-Up data, analyses of reference profiler comparison data from MnROAD (Perera, 2006), and further development of a Butterworth filter for use within ProVAL. Five important proposed enhancements to the specifications in the CPAR report are:

1. Data from the 2004 FHWA Profiler Round-Up and other comparisons of reference profilers further justify the correlation thresholds suggested in the CPAR report. (See “Cross Correlation” below.)
2. The Butterworth filter described in the CPAR report was improved for integration into ProVAL. We plan to use the improved filter to isolate the wavebands of interest for cross correlation analysis. (See “Filtering” below.)
3. The procedure for interpolating one profile to have a compatible recording interval with another for cross correlation analysis includes up-sampling to avoid penalties due to smoothing effects. (See “Cross Correlation” below.)
4. The “Cross Correlation” section, below, demonstrates the penalty to the profile agreement score that results from non-linear phase shift.
5. The benchmark profile measurements will be made by a device that functions on the same principle as the rod and level, but with an optical footprint. (See “Benchmark Profile Measurement” below.)

The rest of this document describes six aspects of the Benchmark Testing Plan: (1) test sections, (2) field procedures, (3) reporting of results, (4) rating of agreement using cross correlation, (5) profile filtering methods, and (6) benchmark profile measurement. At this stage, the field procedures, reporting of results, rating of agreement, filtering methods and benchmark profile measurement methods are considered to be finalized.

Pre-Approval

Pre-approval is required for a candidate refernece profiler to participate in the reference evaluation. The equipment manufacturer or vendor shall submit documentation to the FHWA that consists of a minimum of ten test runs of the equipment over one 161-m (528-ft) long section of asphalt concrete surfaced pavement and one 162-m (528-ft) long section of concrete surfaced pavement. The candidate shall provide an electronic copy of the profiles in the ASTM E2560 *ppf* file format or ERD format. The test runs shall show compliance with cross correlation of IRI filter output requirement of 0.98 for repeatability. On each surface type, cross correlate each of the ten profiles to each of the remaining nine. (This represents 45 comparisons.) The repeatability “score” for each trace is the average of all 45 cross correlation values. **A score of 0.98 or greater is required on each pavement surface in order for the equipment to be allowed to participate in the reference profiler evaluation.**

Test Sections

Properties

The dominant criterion for selecting test sections is macrotexture type. Ideally, benchmark testing would cover a diverse set of texture types. The CPAR report specified testing on six surface textures, including

1. Dense graded asphalt with small aggregate: This provides a section with very little macrotexture. The maximum aggregate size should be 9.5 mm (3/8 in) or less.

2. A fresh chip seal: This provides a section with isotropic texture, with emphasis on the short wavelength end of the macrotexture range. A fresh chip seal also contains "positive texture," in that the excursions from the nominal road elevation are upward.

3. Stone matrix asphalt (SMA) or open graded asphalt with a large maximum aggregatge size: This provides a section with isotropic and negative texture, with emphasis on the long wavelength end of the macrotexture range. If SMA is selected, it should have a maximum aggregate size of 12.7 mm (1/2 in) or larger. If an open graded asphalt is selected, aggregate with a maximum size of 25.4 mm (1 in) or less is preferred.

4. Transversely tined jointed concrete: Transverse tining provides the most common example of transverse texture in concrete pavements. Any typical joint spacing is permitted, but the section must include saw-cut joints without protruding sealant. The tining and joints provide examples of "negative texture," which pose a challenge to the bridging qualities of a device's footprint.

5. Longitudinally ground concrete: This provides an example of longitudinal texture. The entire section should be ground, which is likely to also provide a very smooth surface. In place of a ground section, the experiment may include a concrete pavement with a drag texture.

6. Longitudinally tined concrete: This provides another example of longitudinal texture, with depth and lateral dimensions that are unique compared to longitudinal grinding. Longitudinal tining has posed the greatest challenge to modern profilers.

Using this mix of diverse surface textures, or one that includes the same range of macrotexture types, is very important. A reference profiler that demonstrates acceptable performance on this mix of surface textures is expected to provide credible measurements over a broad range of conditions.

Changes in texture over a given length of pavement present an additional factor in profile measurement other than the texture itself. Thus, we prefer samples of each texture type that are at least a tenth mile long. However, we may use a much shorter section to verify profiler operation in the short and medium waveband if a sufficiently long section of a given texture is not available. Verification of long wavelength measurement requires at least one test section that is two tenths of a mile (or more) long.

The benchmark testing will emphasize profiler performance on smooth pavements. We anticipate that most reference profiler measurements will take place on smooth and medium smooth pavements, as specified in AASHTO PP 49. Further, very smooth pavements with coarse macrotexture pose a significant challenge to road profilers. Thus, it is most important to test candidate reference device repeatability and accuracy on fairly smooth pavements.

Testing Locations

The initial round of benchmark testing will take place at the MnRoad facility near Albertville, MN. The six test sections will be selected in the days prior to the experiment to

match the properties described above. The dense graded asphalt section will be 366-457 m (1200-1500 ft) long. To the extent possible, the other test sections will be approximately 137-162 m (450-530 ft) long.

Field Procedures

Scheduling

The FHWA contractor will coordinate testing so that as many of the candidates can participate in the evaluation as possible. Access to each test section will be provided by appointment only, and we will observe all the official testing. As such, participants must arrive at the designated test sections for their appointment, and may not encroach on other appointments. (That is, rescheduling and extra time must not interfere with other appointments, but each appointment will provide a sufficient amount of time. For scheduling purposes, we will ask each candidate how much time they need to set up and perform six high-quality runs on a test section.)

We will stay in contact with all the candidates in the days before testing and during test days. That will allow us to adjust the scheduling as needed to accommodate interruptions caused by bad weather.

Only one candidate may occupy a test section at a time, so that they do not interfere with each other. We will operate only as many test sections as we have people to observe the testing. No measurements will be permitted after hours, and no data will be accepted from unscheduled or unobserved visits to the test sections.

Test Section Layout

Testing will cover only one longitudinal strip (i.e., “longitudinal track”) of pavement. The longitudinal track of interest will usually appear on the right side of the lane. Clear markings will appear at the longitudinal position of the start and end of the test section using paint or dull tape. On most test sections, the markings will be at an undisclosed distance 137-162 m (450-530 ft) apart. (The study includes one longer test section.)

The lateral position of the longitudinal track of interest will be a known position that is 15.24-45.72 cm (6-18 in) to the side of the marking. (The value will be set before scheduling of field tests, disclosed to all the participants, and will not change.) Note that we will specify the center of the lateral position of interest, but will measure a strip 70 mm (2.76 in) wide with the benchmark profiler.

If a candidate needs markings beyond those provided, they must describe them while scheduling the testing. Candidates will not be permitted to make permanent markings on the test sections. We will try to make sure that participants have the markings they need to make their measurements, but all required markings will be considered part of the measurement effort required for operation of the device.

One longitudinal distance measurement calibration section will be provided at MnRoad. On this section, we will provide markings that are 304.8 m (1000 ft) apart. The distance will be measured with a steel tape, pulled taut every 30.48 m (100 ft), and corrected for temperature.

Testing Sequence

Before the testing begins, the operators of each candidate device must provide a FHWA contractor staff member an overview of the operational procedures of the device. This includes (1) start up procedures, such as device assembly, calibration and system health checks, and software start-up; (2) measurement procedures; and (3) the process of finalizing a run and offloading data in ERD format or ASTM E 2560-07 format. The demonstration does not need to take place on a test section of interest for the benchmarking, and the run will not be included in the analysis, but the run must cover at least 450 ft. A short written description that provides an overview of the equipment including calibration procedures, measurement procedures, principles of operation, dimensions of the equipment, weight of the equipment, and cost of the equipment must be provided via e-mail at least two weeks before the scheduled test date. An example data file, either in ERD format or conforming to ASTM E2560-07 format, shall be submitted at least three weeks before the test date

The FHWA contractor will observe all official runs. Candidate device operators are expected to make exactly six runs on each section and submit data from all of them. Aborted runs are discouraged and will be recorded by the observers of the testing. An operator may abort up to two runs but may not exclude a run after reaching the end of the test section.

Data Submittal

Candidates must submit all data within a short time (i.e., a few minutes) after completing the measurements at each test section, and may not submit data after leaving the section. Data files must identify the profile point that corresponds to the section start and the longitudinal recording interval. Files shall be named using the first four characters to identify the profiler, the next two characters to identify the test section, and the next two to identify the repeat number. The four characters to identify each profiler and the two-character identifier for each test section will be provided before testing commences. Data must be provided SI units in ERD or ASTM E 2560-07 format.

Reporting

Benchmark Test Evaluation Report

The FHWA contractor will provide the equipment manufacturer with a “Benchmark Test Evaluation Report” within 56 calendar days of completion of the testing. Appendix A provides a prototype report. The report describes the performance of the device on each test section. The FHWA contractor will forward copies of all Benchmark Test Evaluation Reports to the FHWA.

The Benchmark Test Evaluation Report includes:

- Test Section and Device Identification: This section describes the candidate reference device and the test section. It also provides the candidate device recording interval, the up-sampling interval for cross correlation analysis, and the rationale for the use or omission of the 250 mm moving average within IRI calculations.

- Summary Results: This section provides pass/fail ratings of profile repeatability, profile accuracy, and longitudinal distance measurement accuracy. This section also provides composite repeatability and accuracy scores as defined below in four wavebands (IRI, long, medium, short).
- Detailed Results: This section provides all the results that affect the composite scores and pass/fail ratings. The detailed results include longitudinal distance measurement error for each run, cross correlation to the benchmark profile measurement from each run in each waveband, and cross correlation between all pairs of repeat measurements in each waveband and for all subsections in the short waveband.
- Special Observations: This section provides observations of interest to the device manufacturer. For example, it will report cases in which correcting longitudinal distance measurement error or eliminating a small number of repeat measurements would significantly improve composite repeatability or accuracy scores.
- Auxiliary Information: This section provides other information of interest about the device, including a description of the overall measurement concept, expected unit cost, start up and field calibration procedures, demands on the operator, and the time required per run. Time per run includes the entire "loop time" including the time requirement to make the measurement, the time needed to return to the section start, and the time needed to initialize the device. Note that if the operator measures longitudinal distance using a device other than the candidate reference profiler (e.g., a steel tape or a measurement wheel), that activity will be treated as part of the measurement effort.

A composite repeatability score for a given waveband is the average cross correlation level of all possible pairs of repeat measurements. In the IRI, long, and medium wavebands, 6 repeat measurements corresponds to 15 individual profile comparisons and the composite score is the average of the 15 correlation values. In the short waveband, cross correlation is performed on four subsections within a given test section. The composite repeatability score is the average of the composite repeatability scores for each of the four subsections.

A composite accuracy score for a given waveband is the average cross correlation level to the benchmark profile. In the IRI, long, and medium waveband, 6 repeat measurements corresponds to 6 individual profile comparisons and the composite score is the average of those 6 correlation values. In the short waveband, cross correlation is performed on four subsections within a given test section. The composite accuracy score is the average of the composite accuracy scores for each of the four subsections.

Benchmark Test Evaluation Summary

Upon completion of the entire testing series, UMTRI will provide each equipment manufacturer with a "Benchmark Test Evaluation Summary." Appendix A provides a prototype. The Summary provides a concise snapshot of a device's performance over all of the test sections visited. The Summary also provides a refined report of the auxiliary information described above that may impact a DOT's decision to purchase a device and

adopt it as their reference profiler. (This includes cost, measurement principle, measurement effort, required operator proficiency, etc.) The Summary is subject to review by the FHWA and the Pooled Fund Group, and it serves as the basis for a final report of device performance.

Disputes

Equipment manufacturers must direct disagreements with reported results directly to the FHWA, and the FHWA will provide the response. UMTRI will not provide an official response to verbally communicated disputes or disputes described through e-mail communication with UMTRI. All disputes and the corresponding response will be communicated to the other participants, and any change to the official criteria will be applied uniformly to all participating devices.

Equipment manufacturers have the opportunity to review the final version of this document (at the end of Task B) for at least three weeks before scheduled testing. Disputes with the contents of the testing and analysis plan will be considered much less persuasive after the results of the testing are provided.

We strongly encourage equipment manufacturers to test their profile repeatability and longitudinal distance measurement accuracy before official benchmark testing. The benchmark IRI values and longitudinal distance values will be provided in the reports, but the benchmark profiles will not be provided to the candidates.

Benchmark Profile Measurement

A detailed description of the Benchmark Profile can be found in the Benchmark Profiler Field Manual.

The benchmark profiler uses the same measurement concept as a rod and level. A rod and level establishes the elevation at a given location by measuring the distance along a vertical rod beneath a stable reference height. The benchmark profiler will act similarly but include modifications to overcome the slow measurement speed, long recording interval, and inappropriate footprint of the surveyor's rod in its traditional form. Appendix B provides several photos of the benchmark profiler.

Kernel

Figure B-1 shows the "kernel" of the benchmark profiler mounted on the three-wheeled, motorized cart. In the photo, the front end of the cart appears at the top and the rear end appears at the bottom. The kernel includes three instrumentation systems:

1. Body orientation and vertical position: A sweeping laser, mounted on a ground-based tripod positioned behind the cart, defines the stable reference plane above the road surface. The beam from this sweeping laser is projected onto three screens mounted on the kernel. A machine vision camera senses the beam on the screens to establish the height as well as the pitch and roll angles of the kernel relative to the reference plane. Two aft screens are present side by side for detection of roll angle (i.e., rotation about the longitudinal axis), and the third screen is separated longitudinally for detection of pitch angle (i.e., rotation about the lateral axis). The

vertical position of the laser sweep at a reference (central) lateral position between the aft screens establishes the reference height.

2. Vertical range to road: A RoLine laser measures the vertical distance (i.e., range) between a reference location on the kernel and the road surface. The RoLine provides several values over a wide footprint. A bridging algorithm will reduce the values that fall within a given area of interest to a single range value.

3. Body location on the ground: A second machine vision camera detects the lateral position and yaw angle of the cart relative to a nylon-coated steel tape fixed to the road. These readings provide feedback to a steering control system that maintains a consistent lateral position of the kernel as the host cart moves forward.

Like the level in a rod and level measurement system, the sweeping laser provides a consistent vertical reference plane for the device. The device establishes the distance from the reference plane to the road surface using two dimensions. The first is the vertical position of the sweeping laser on the main screen compared to a reference point on the device kernel. The second dimension is the distance from the reference point to the road surface, which is established by the vertically oriented ranging laser. Longitudinal distance is established using the steel tape.

Host Cart

The kernel described above rides on a slow-moving cart that also carries a drive motor, steering and drive control apparatus, DC power, and the data acquisition system. The cart also carries a canopy to help provide consistent background light for the cameras and helps avoid swell on the device kernel that could be caused by fluctuations in temperature.

Figure B-2 shows a view of the un-shrouded host cart from the rear. The cart is approximately 88 cm wide, 115 cm long, and 74 cm high. Three wheels support the cart: a drive wheel at the center rear of the cart and two steered wheels in the front corners. The host cart provides a rolling platform for the device kernel. It also carries batteries, power supplies, ethernet switches, and other electronics needed to support the RoLine and two cameras, as well as an instrumentation rack, a control panel, controller boards for steering and propulsion, and a data acquisition system (DAS). Overall, the device weighs about 182 kg (400 lbs).

Four sealed, lead acid batteries supply power to the cart. Two of them provide a 12 V supply in parallel, and the other two provide 24 V in series. The batteries are recharged using a 110 V, 10 Amp battery charger (or using jumper cables and a 12 V vehicle battery) via three custom 12 V outlets. (See Figure B-3.)

During regular operation, the host cart is enclosed by an insulated cover equipped with multiple cooling fans for expelling heat generated by the electrical systems.

Propulsion

An electric wheel chair motor propels the cart at the rear wheel in either forward or reverse. The drive wheel is made of hard rubber, machined to a diameter of 146 mm (459 mm per revolution). In manual mode, the operator controls speed (and steering) using a

hand-held joystick. The controller program constrains the maximum speed to approximately 760 mm/sec. During automated data collection, the DAS commands the cart to move at a forward speed of 152.4 mm/sec. Under both manual and DAS modes, speed control is achieved using proportional-integral-derivative (PID) control and a quadrature encoder attached to the main motor shaft. The encoder provides 500 counts per revolution.

The motor specifications suggest that the device will be capable of sustained operation on grades of up to 5 percent.

Cart Orientation and Vertical Position

A rotating laser provides a stable reference plane for the cart. A Cognex vision system measures the height and orientation of the device kernel relative to the reference plane by analyzing the image of the laser beam as it is projected on three screens. The system includes an InSight Micro programmable camera and special image processing routines. (See Figure B-1.)

Screen Image

Figure B-4 shows an image captured by the vision system of a laser sweep across the three screens on the device kernel. Since the exposure time for each image encompasses the entire sweep, the laser spot appears as a line on each screen. For each segment of detected light, the vision system derives its position (height and slope) of the corresponding screen by defining a best-fit line along the transition between light and dark pixels above and below each line. The camera's algorithm defines each of these lines by identifying their end points. The end points of the center line of the laser image on each screen is determined by averaging the end points of the upper and lower transition lines. Finally, the four end points for lines on the aft screen are used to determine a best-fit line for the aft plane. Then additional, real-time, imbedded processing routines in the camera derive three quantities relative to the laser reference plane:

1. Kernel height: This is derived by determining the intersection of best-fit line on the aft plane with a vertical line through the center of the image.
2. Kernel roll angle: This is derived using the slope of the best-fit line on the aft plane.
3. Kernel pitch angle: This is derived by comparing the kernel height as determined in step (1) with the kernel height determined in a similar fashion using the line of the forward plane (inner screen).

The system collects and processes these images asynchronously, but at a rate expected to be approximately 20 Hz. The overall image covers an area 8 inches wide and 5.5 inches high, and 640 pixels wide and 480 pixels high. This permits vertical resolution of each pixel on the order of 0.3 mm. However, the ability to judge a degree of illumination in each pixel and the use of a linear fit over a significant width permits the system to resolve height to a much finer precision level.

The camera lens is outfitted with two special filters that limit the incoming light with a pass-band that is 13 nm wide. A light tunnel with dark sides further reduces contamination of the images by ambient light. (See Figure B-2.) Successful detection of the laser image as

it sweeps past the screen also depends on careful control of the gain applied to the light sensed by the camera's detector, as well a real-time control of camera exposure time.

Trigger

As shown in Figure B-2, the cart includes a second light tunnel. A silicon photo diode in this light tunnel detects the imminent arrival of the rotating laser beam on the device kernel. (See Figure B-5.) A Fresnel lens focuses the incoming light toward the diode to help guarantee that the beam is detected. The system high-pass filters and amplifies the signal from the diode. As soon as the laser beam is detected, a timing pulse is provided to the data acquisition system. After a very short delay, the system triggers the Cognex camera to collect an image of the screens.

Sweeping Laser

The sweeping laser is a Hamar Laser L-740. This unit sweeps 5 times per second. It projects a collimated beam about 4.06 mm in diameter. The laser diode projects light at a wavelength of 658 nm, and projects 3 mW of power. The specifications list laser plane flatness of 0.5 arc sec and beam stability of 0.2 arc sec/hr/degree F. More importantly, measurements of the laser beam by the vision system described above confirmed stability of the beam of 0.08 mm at a distance of 37 m when the cart was stationary.

Laser Set-Up

A 160-m test section will be measured in 3-4 segments, depending on lighting conditions. In each set-up, the laser reference plane will be established with a roll angle relative to gravity at or near zero. In addition, the plane will roughly follow the grade of the road over the segment of interest (at a known tilt angle). The overall "grade" of the reference plane in each set-up will be used to resolve the profile elevation values to a flat reference plane. For the initial experiment, sub-section endpoint elevation values will be measured using a conventional rod and level survey to verify the sweeping-laser established height differences.

Vertical Range to the Road

Vertical range to the road surface is measured using a RoLine 1130 laser sensor. The light projected by the RoLine is fixed within the device kernel, and it is constrained to the same plane as the side-by-side screens used to detect the laser reference plane.

The RoLine is mounted 325 mm above the ground plane. At this standoff height it provides up to 150 data points spread out over a width of 110 mm. The 110-mm wide footprint is arranged to contain a 70 mm wide track of interest, a nylon-coated steel tape (for reference), and some extra width on the outside to accommodate wander of the cart.

Figure 1 shows the layout of the track of interest and the steel tape within the laser footprint when the lateral control is in its neutral position (i.e., zero lateral offset). The control system, described below, steers the cart to ensure that the track of interest and the left edge of the steel tape appear within the RoLine footprint. In the neutral position, the footprint includes 13 mm of extra width on either side of the track of interest, and will just

barely include the entire width of the steel tape. This provides for 13 mm of wander without missing any of the track of interest or the left edge of the tape.

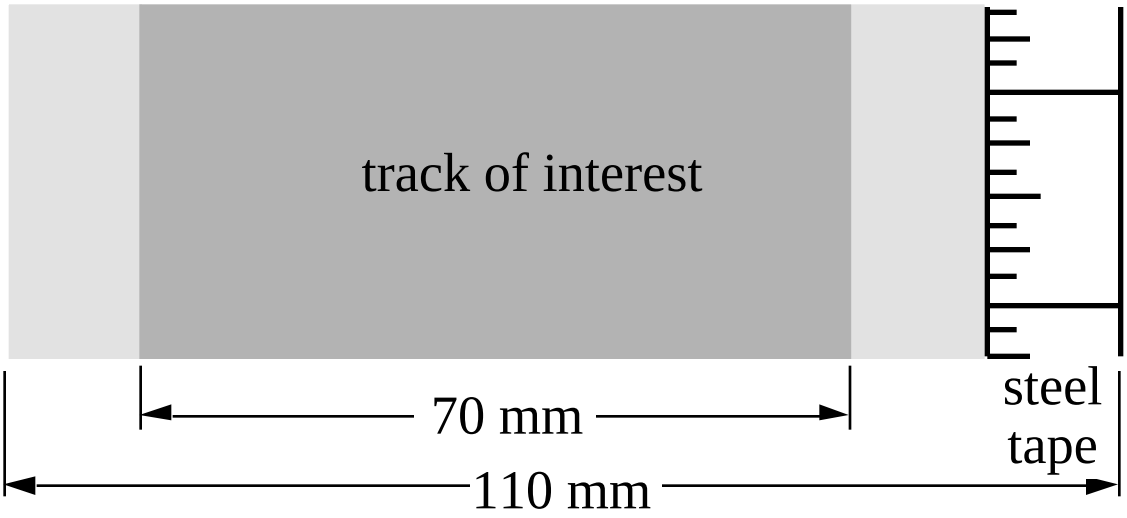

Figure 1. Layout within the RoLine footprint.

The lateral offset from the steel tape determines the data points that fall within the track of interest. These 95 data points range from 13 mm to 83 mm to the left of the left-most ridge between the steel tape and the pavement. Typically, the location of this ridge within the footprint is obvious. Figure 2 provides an example.

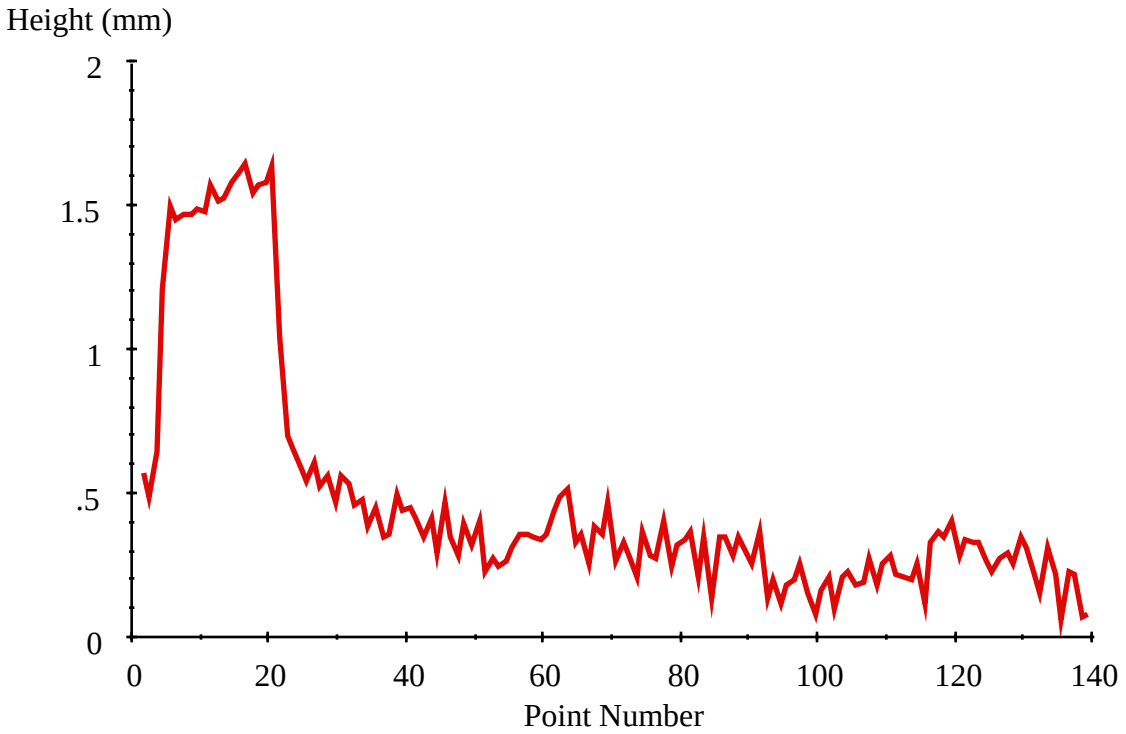

Figure 2. Sample RoLine output.

Each output point provides the distance from a reference point on the device kernel to a point on the road in the coordinate system fixed within the device kernel. These values are transformed into a reference coordinate system using the relative pitch and roll angles of the kernel, which are measured as described above. More importantly, the precise longitudinal placement of each RoLine reading on the ground is derived using the overall cart longitudinal position and the projection to the ground of the RoLine footprint using pitch angle. Further, the range within the RoLine footprint of the track of interest is estimated using roll angle to guide the search for the steel tape inner ridge.

The RoLine laser provides 3000 "lines" per second at a constant rate. Since the device will move very slowly (152.4 mm/sec) this is an excessive amount of data, corresponding to nearly 20 readings per millimeter. Each line is reduced to a single height value using the bridging filter described in the "Filtering" section of this Plan.

Cart Location on the Ground

A nylon coated steel tape fixed to the test section parallel to the longitudinal track of interest provides a location reference for the cart. A Cognex vision system measures cart yaw angle, lateral position, and longitudinal position relative to the tape. The system includes a downward facing InSight Micro programmable camera and special image processing routines.

Figure B-6 provides a sample image of the ground and steel tape from the camera during automated operation. The image processing routines search the captured image for a section of the image that best correlates to a "memorized" target image of a segment of steel tape. (See Figure 3.) This determines the lateral, longitudinal and angular position of the chosen segment within the capture image.

Figure 3. The target image.

Whenever the appropriate range of numbers appears in the captured image, the sample pattern is found with a very high correlation score. If the appropriate range does not appear in the image, the program still detects the tape, but at a lower correlation score, because, while the proper digits do not appear, the general hash mark pattern on the captured image and the hash mark pattern in the target image still correlate well. In the latter case, the lateral position and yaw angle are correct, but the longitudinal position is not. The camera program provides lateral position, yaw angle, longitudinal position and the correlation score to the DAS, regardless of the correlation level.

The vision system provides readings asynchronously (the search routines tend to take longer when the actual target is not present) at approximately 20 Hz.

Longitudinal Distance

In post processing of the cart location data, those longitudinal measures accompanied by a high correlation score will be used to establish the longitudinal progress of the cart in one-foot increments. Between each of these increments, the longitudinal position will be determined to much finer resolution using a 2000 pulse-per-revolution encoded driven directly by the drive wheel axle (as opposed to the encoder mounted on the motor shaft which is used for speed-control feedback).

Body Lateral Position/Steering Control

A linear actuator steers the host cart through a conventional Ackerman steering system. (Figure B-7 provides a top view of the steering linkages.) A PID servo controller board controls the actuator. In manual operation, the steering (and drive) commands are provided using the hand-held joystick.

During automated data collection, the DAS provides steering commands to a PID controller in order to maintain a consistent lateral position relative to a nylon-coated steel tape fixed to the ground. The cart's lateral offset (from the desired position) and yaw angle are measured by the machine-vision system described above. Within the camera's program, these measures are processed to determine the appropriate steering command using kinematics of the cart, known dimensions, and an appropriate time constant for eliminating lateral position errors. This command, along with the lateral position and yaw angle data (as well as longitudinal position and a correlation score), is sent to the DAS, which, in turn, forwards the steering command to the controller board. During indoor testing, this automatic steering system maintained the desired lateral position of the cart to within 3 mm and yaw angle to within 1 degree.

Cross Correlation

This section describes the application of cross correlation for rating agreement between profiles. In particular, it defines the details of the calculation procedures for rating agreement between multiple measurements by candidate reference profilers over the same segment of road (i.e., repeatability) and rating agreement between candidate reference profiler measurements and benchmark profile measurements (i.e., "accuracy").

Thresholds

A reference device must demonstrate accuracy on a given test section by correlating to the benchmark profile with an average rating over 6 profile measurements of at least:

0.98 for IRI filter output,

0.98 in the long waveband,

0.98 in the medium waveband, and

0.94 in the short waveband.

The "Filtering" section of this document defines the long, medium, and short waveband and describes how they will be isolated. A reference device must also demonstrate

composite repeatability over 6 measurements above the same thresholds. Appendix C provides justification for these thresholds.

Calculation Procedure

Cross correlate a profile from a candidate device to a benchmark profile measurement in a given waveband of interest as follows:

Step 1: Identify the benchmark profile.

Designate the benchmark profile (Q), recorded at a constant interval of δ_Q. The profile shall begin at a longitudinal reference location of "zero," which corresponds to the section start. Denote each profile point with an indexed value, starting a Q(0) and ending at $Q(N_Q)$, where $L_Q = \delta_Q \bullet N_Q$.

Step 2: Identify the candidate profile.

Designate a candidate profile (P), recorded at a constant interval of δ_P. Crop the profile (P) so that it begins at the test section starting point. Terminate the profile at the test section end point. Denote each profile point in the cropped profile with a subscript, starting a P(0) and ending at $P(N_P)$, where $L_P = \delta_P \bullet N_P$.

Note: The data file must identify the profile point that corresponds to the section start, the profile point that corresponds to the section end, and the recording interval.

Note: The value of L_P and L_Q will not necessarily be equal, because of potential incompatibility in longitudinal distance measurement.

Step 3: Filter and up-sample the benchmark and candidate profiles.

Step 3a: Pad the profiles by reflecting both vertically and horizontally about the end points. For the benchmark profile:

$Q(-n) = 2 \bullet Q(0) - Q(n)$

$Q(N_Q + n) = 2 \bullet Q(N_Q) - Q(N_Q - n)$, where n = 1 through N_Q.

For the candidate profile:

$P(-n) = 2 \bullet P(0) - P(n)$

$P(N_P + n) = 2 \bullet P(N_P) - P(N_P - n)$, where n = 1 through N_P.

This will nearly triple the length of the profiles.

Step 3b: Filter the profiles. (See "Filtering.")

Step 3c: Crop the filtered profiles to include the range they had before they were padded. Retain points in the benchmark profile from index values of 0 through N_Q. Retain points in the candidate profile from index values of 0 through N_P.

Step 3d: Up-sample the profiles to a common sample interval δ. If possible, select a value for δ such that both δ_Q and δ_P are integer multiples of it. If this is not possible or the value of δ would have to be less than 0.04 in (1 mm), up-sample both profiles to a recording interval of 0.2 in (5.08 mm).

Note: The filtered and up-sampled candidate profile (p) now includes N_p+1 data points with index values that range from 0 to N_p, where:

$$N_p = \text{int}(N_P \bullet \delta_P/\delta)$$

(The "int" function truncates the value of its argument to an integer value.)

Note: The filtered and up-sampled benchmark profile (q) now includes N_q+1 data points with index values that range from 0 to N_q, where:

$$N_q = \text{int}(N_Q \bullet \delta_Q/\delta)$$

Step 4: Cross correlate the candidate profile (p) to the benchmark profile (q) several times over a range of longitudinal offsets.

Do this by shifting the longitudinal distance referencing for the candidate profile (p) by various amounts, ranging from $-X_{off}$ to X_{off}. An index value of "0" denotes the section start. When the candidate profile (p) shifts longitudinally by a distance of (or near) in the downstream direction, the new index value of the first point is:

$$N_{off} = \text{int}(X_{off}/\delta)$$

(The true shift is then $N_{off} \bullet \delta$.)

When the candidate profile (p) shifts upstream by the same distance, the first point has an index value equal to the opposite of N_{off}.

Step through the possible range of index offset values from $-N_{off}$ to N_{off} and cross correlate the candidate profile (p) to the benchmark profile (q). Cross correlate over the overlapping portion of the profiles at each step.

For an offset index value of "m", the correlation covers a range of index values from:

$$N_{start} = \max(m, 0)$$

to

$$N_{end} = \min(N_p - m, N_q)$$

As a function of the offset value, the correlation is:

$$\rho(m) = \frac{1}{\max(\sigma_p, \sigma_q)^2} \sum_{i=N_{start}}^{N_{end}} \left[(p(i+m) - \mu_p) \bullet (q(i) - \mu_q) \right]$$

Where:

$$\mu_p = \frac{1}{N_{end} - N_{start} + 1} \sum_{i=N_{start}}^{N_{end}} p(i)$$

$$\mu_q = \frac{1}{N_{end} - N_{start} + 1} \sum_{i=N_{start}}^{N_{end}} q(i)$$

$$\sigma_p = \frac{1}{N_{end} - N_{start} + 1} \sum_{i=N_{start}}^{N_{end}} \left(p(i) - \mu_p \right)^2$$

$$\sigma_q = \frac{1}{N_{end} - N_{start} + 1} \sum_{i=N_{start}}^{N_{end}} \left(q(i) - \mu_q \right)^2$$

Step 5: Report the maximum correlation level and the corresponding longitudinal offset.

The maximum correlation level is the highest value of ρ. For the index "m" at which the maximum occurs, the offset is $m \bullet \delta$.

The steps listed above apply to cross correlation in the IRI, long and medium wavebands. In the short waveband, the profiles will be further cropped into sub-sections 32.2 m long between steps 3 and 4. Analysis in the short waveband will cover up to four sub-sections within a given profile measurement.

Steps 1 through 5 produce a correlation value for a single pair of measurements. The criteria for profile accuracy places threshold values on composite correlation, which is the average over comparisons of each repeat candidate profile measurement to the benchmark profile within a given waveband.

To produce a repeatability score, all possible pairs of repeat measurements from the candidate profiler should be cross correlated. To do this, apply the steps listed above to every possible pair of repeat measurements within the waveband of interest. This is done by (temporarily) treating one of the profiles as the benchmark profile. It is likely that all of the repeat measurements will have the same recording interval. In this instance, up-sampling is not performed.

Filtering

Profile comparisons will be conducted in four wavebands of interest: (1) the IRI waveband, (2) a long waveband, (3) a medium waveband, and (4) a short waveband.

IRI Waveband

This "IRI waveband" corresponds to the response of the filters that make up the IRI algorithm. This filter includes three parts:

1. application of a moving average with a 250 mm (9.84 in) base length (if required),
2. conversion of the profile to slope, and
3. application of the Golden Car simulation of suspension stroke.

Sayers (1995) provides the details of the IRI calculation algorithm.

Other Wavebands

A set of Butterworth filters will isolate the long, medium, and short wavebands. The filtering procedure is the same as the one used in ProVAL (version 2.7 and later), as described in Appendix F. The filter set includes both high-pass and low-pass third-order Butterworth filters. These are cascaded using a first order Butterworth and a complementary second order filter. The procedure applies each filter in both directions, to reverse the phase distortion caused by each component. This doubles the order of the filter to six. The profile comparison process for this project applies the filters only after padding the profiles, to help reduce problems with initialization (see "Cross Correlation").

The filters will isolate the short waveband using a high-pass filter cut-off value of 1.6 m (5 ft) and rely on the bridging filter, described below, for low-pass filtering. Comparison of the short waveband only covers profile segments 32.2 m (105.6 ft) long, to reduce the penalty to correlation caused by small differences in longitudinal distance measurement. The filters will isolate the medium waveband using a high-pass filter cut-off value of 8 m (25 ft) and a low-pass filter cut-off of 1.6 m (5 ft).

The filters will isolate the long waveband using a high-pass filter cut-off value of 40 m (125 ft) and a low-pass filter cut-off of 8 m (25 ft) on all test sections that are approximately 0.16 km (0.1 miles) long. On test sections 0.32 km (0.2 miles) or longer, the high-pass filter cut-off value will be increased to 67 m (220 ft). A long test section and a larger cut-off value provide an opportunity to verify profiler performance on the long end of the waveband of interest (Karamihas, 2005).

Bridging Filter

The filtering applied for the purposes of profile comparison includes no special algorithm for bridging over narrow concave profile features or negative surface texture. However, the benchmark profiler applies a bridging algorithm to its measurements of road surface height as part of the profile measurement and calculation algorithm. This affects profile content in the wavebands of interest and strongly affects the short waveband.

The bridging filter is first applied to each "line" provided by the RoLine sensor over the 70 mm track of interest. This filter seeks the height that represents an average "protrusion" into the space above the pavement of a given amount. (This is a simple model of a heavily compliant solid piece of material that is penetrated by the road so that a set volume is

displaced.) This filter is described in the CPAR report. for this experiment, the bridging filter “depth” is set to 0.7 mm (0.028 in).

Once the bridging filter is applied across each set of RoLine readings in the transverse direction, it is applied again to a series of readings that appear within a longitudinal distance of 76.2 mm (3 in).

Appendix A: Prototype Reports

This appendix provides sample reports of equipment performance.

Benchmark Test Evaluation Report

Test Section: <<Describe the test section location and texture type.>>

Date: <<List the test date(s) and time window.>>

Device: <<Provide the device make and model.>>

Operator(s): <<Name the operator(s) and their organization.>>

Recording Interval: <<List the recording interval in the same units and precision level that was provided in the data file(s).>>

Use Moving Average: <<List "Yes" if the 250 mm moving average should be applied for IRI calculations, "No" if not.>>

<<Describe the reasoning for omitting the moving average if that is the case. For example: "A notch appeared in the PSD plots at a wave number of 4 cycles/m." >>

Up-Sampling: For comparison to the benchmark profile measurement, data were up-sampled to an interval of <<x.xx>> mm.

Results for Profile:

	Repeatability		Accuracy	
Waveband	Score	Result	Score	Result
IRI	<<0.99>>	<<P/F>>	<<0.99>>	<<P/F>>
Long	<<0.99>>	<<P/F>>	<<0.99>>	<<P/F>>
Medium	<<0.99>>	<<P/F>>	<<0.99>>	<<P/F>>
Short	<<0.95>>	<<P/F>>	<<0.95>>	<<P/F>>

<<The table shall provide the composite repeatability and accuracy score for each waveband, and a statement of whether each score meets or does not meet the relevant criterion.>>

Result for Longitudinal Distance: <<P/F>>

<<State pass of fail above. List the range of percent error here.>>

Run Log, DMI Results:

Run	Start Time	End Time	IRI (mm/km)	Percent Error	Length (m)	Percent Error
1						
2						
3						
4						
5						
6						

<<Provide the benchmark value for test section length and IRI here.>>

Accuracy Scores:

	Cross Correlation to Benchmark Profile by Waveband						
Run	IRI	Long	Medium	Short, Seg. 1	Short, Seg. 2	Short, Seg. 3	Short, Seg. 4
1							
2							
3							
4							
5							
6							
Ave.							

Repeatability:

Run 1	Run 2	Cross Correlation by Waveband						
		IRI	Long	Medium	Short, Seg. 1	Short, Seg. 2	Short, Seg. 3	Short, Seg. 4
1	2							
1	3							
1	4							
1	5							
1	6							
2	3							
2	4							
2	5							
2	6							
3	4							
3	5							
3	6							
4	5							
4	6							
5	6							
Average								

Special Obseravations:

<<Describe any special observations that explain the results reported above or may help the equipment manufacturer improve their device. Examples include:

- Report cases in which correcting longitudinal distance measurement error improves composite repeatability or accuracy scores significantly.
- Report cases in which excluding up to three repeat measurements would have significantly increased composite repeatability or accuracy scores significantly.
- Describe useful diagnostic information that appears in power spectral density plots or within raw and filtered profile plots.

The first two items above shall not impact official results.>>

Auxiliary Information:

<<Provides other information of interest about the device, including a description of the overall measurement concept, expected unit cost, start up and field calibration procedures, demands on the operator, and the time required per run. Include a short narrative describing the measurement process.>>

Benchmark Test Evaluation Summary

Device: <<Provide the device make and model.>>

Recording Interval: <<List the recording interval in the same units and precision level that was provided in the data file(s).>>

Use Moving Average: <<List "Yes" if the 250 mm moving average should be applied for IRI calculations, "No" if not.>>

<<Describe the reasoning for omitting the moving average if that is the case. For example: "A notch appeared in the PSD plots at a wave number of 4 cycles/m." >>

Up-Sampling: For comparison to the benchmark profile measurement, data were up-sampled to an interval of <<x.xx>> mm.

Overall Results:

Test Section	Accuracy	Repeatability	DMI
Dense Graded AC	<<Pass/Fail>>	<<Pass/Fail>>	<<Pass/Fail>>
12.5 mm SMA	<<Pass/Fail>>	<<Pass/Fail>>	<<Pass/Fail>>
Chip Seal	<<Pass/Fail>>	<<Pass/Fail>>	<<Pass/Fail>>
Transverse Tining	<<Pass/Fail>>	<<Pass/Fail>>	<<Pass/Fail>>
Diamond Grinding	<<Pass/Fail>>	<<Pass/Fail>>	<<Pass/Fail>>
Longitudinal Tining	<<Pass/Fail>>	<<Pass/Fail>>	<<Pass/Fail>>

Profile Accuracy Scores:

	Waveband			
Test Section	IRI	Long	Medium	Short
Dense Graded AC	<<0.99>>	<<0.99>>	<<0.99>>	<<0.99>>
12.5 mm SMA	<<0.99>>	<<0.99>>	<<0.99>>	<<0.99>>
Chip Seal	<<0.99>>	<<0.99>>	<<0.99>>	<<0.99>>
Transverse Tining	<<0.99>>	<<0.99>>	<<0.99>>	<<0.99>>
Diamond Grinding	<<0.99>>	<<0.99>>	<<0.99>>	<<0.99>>
Longitudinal Tining	<<0.99>>	<<0.99>>	<<0.99>>	<<0.99>>

<<Show values of 0.98 and above in bold.>>

Profile Repeatability Scores:

	Waveband			
Test Section	IRI	Long	Medium	Short
Dense Graded AC	<<0.99>>	<<0.99>>	<<0.99>>	<<0.99>>
12.5 mm SMA	<<0.99>>	<<0.99>>	<<0.99>>	<<0.99>>
Chip Seal	<<0.99>>	<<0.99>>	<<0.99>>	<<0.99>>
Transverse Tining	<<0.99>>	<<0.99>>	<<0.99>>	<<0.99>>
Diamond Grinding	<<0.99>>	<<0.99>>	<<0.99>>	<<0.99>>
Longitudinal Tining	<<0.99>>	<<0.99>>	<<0.99>>	<<0.99>>

<<Show values of 0.98 and above in bold.>>

Longitudinal Distance Measurement:

	DMI Error (%)		
Test Section	Average	High	Low
Dense Graded AC	<<0.10>>	<<0.10>>	<<0.10>>
12.5 mm SMA	<<0.10>>	<<0.10>>	<<0.10>>
Chip Seal	<<0.10>>	<<0.10>>	<<0.10>>
Transverse Tining	<<0.10>>	<<0.10>>	<<0.10>>
Diamond Grinding	<<0.10>>	<<0.10>>	<<0.10>>
Longitudinal Tining	<<0.10>>	<<0.10>>	<<0.10>>

Auxiliary Information:

<<Provide other information of interest about the device, including a description of the overall measurement concept, expected unit cost, start up and field calibration procedures, demands on the operator, and the time required per run. Include a short narrative describing the measurement process.>>

Appendix B: Benchmark Profiler Photos

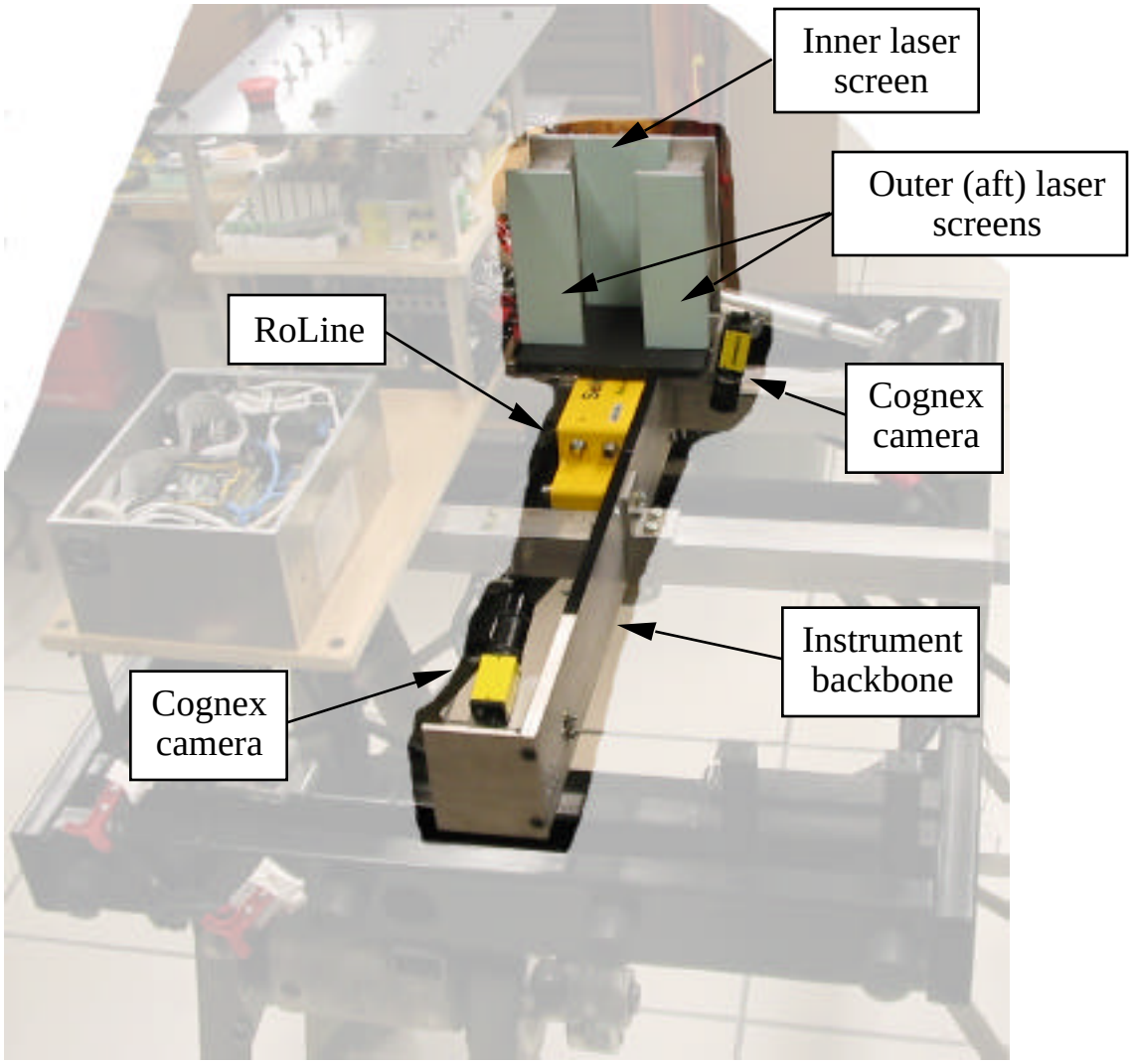

Figure B-1. Benchmark device “kernel”.

Figure B-2. Unshrouded benchmark device.

Figure B-3. Battery charging system.

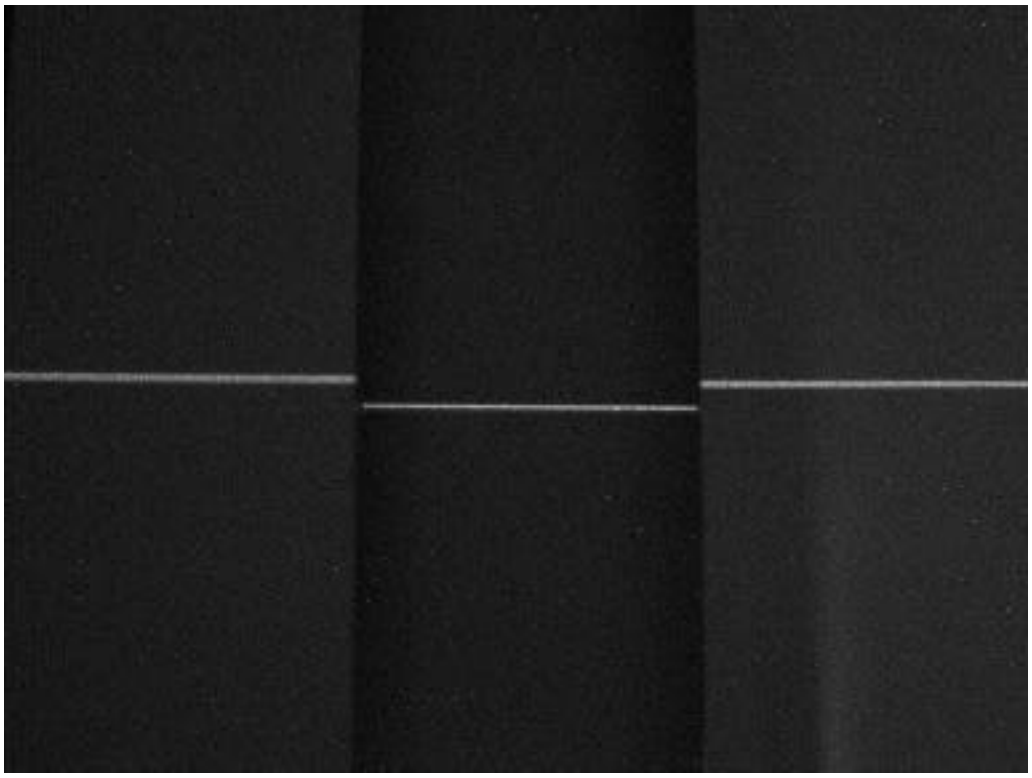

Figure B-4. Laser screen image with a reference line.

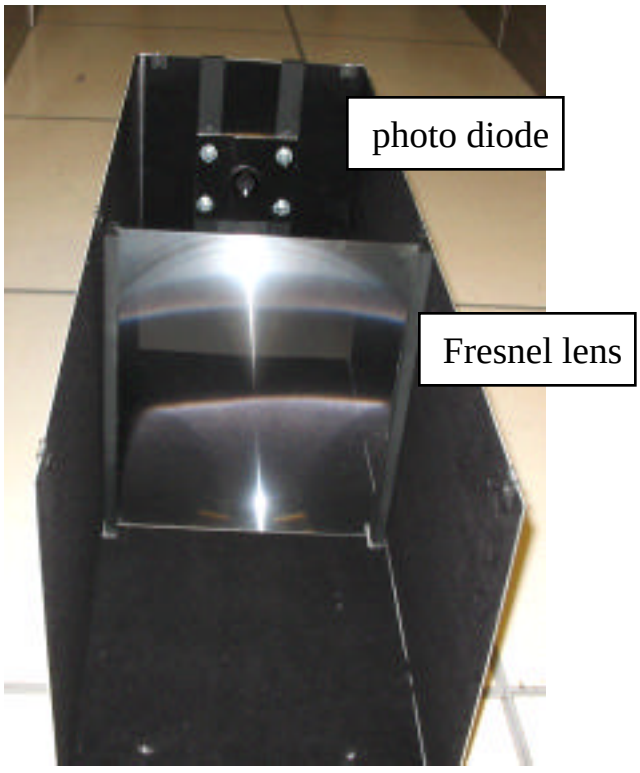

Figure B-5. Light tunnel for camera trigger.

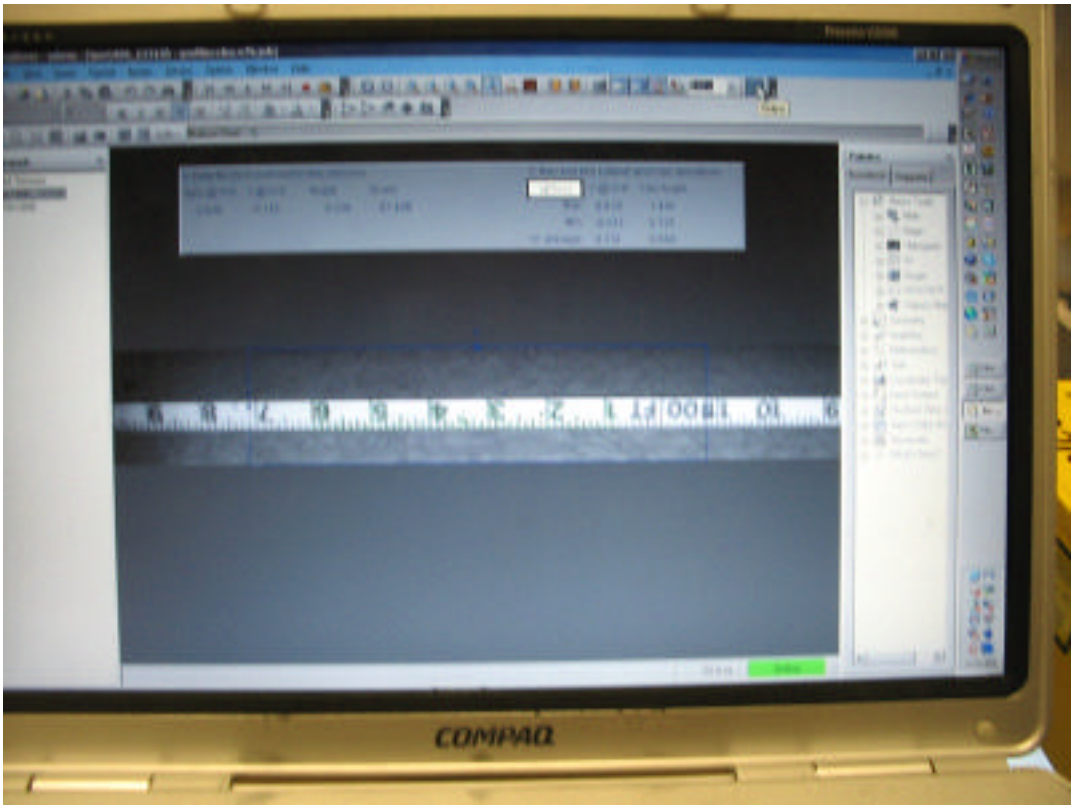

Figure B-6. Steel tape image for steering control.

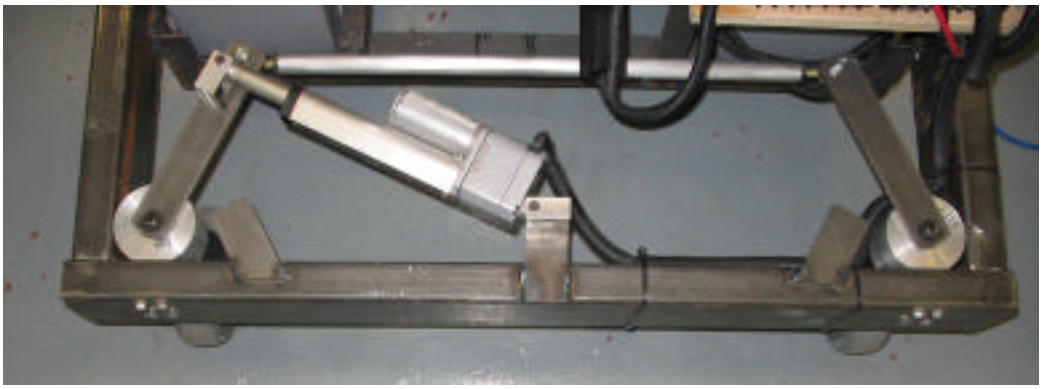

Figure B-7. Top view of steering linkages.

Appendix C: Cross Correlation

This appendix provides background data and analysis in support of the cross correlation calculation procedures, settings and thresholds.

Thresholds

The 2004 FHWA Profiler Round-up provided a large data set that demonstrated a statistical connection between cross correlation and expected agreement in overall IRI for a given test section. Appendix D describes the statistical analysis from the results from the 2004 Round-up. The data show that a given level of cross correlation between two profiles after application of the filters within the IRI algorithm can be linked to an expected maximum disagreement level between the overall IRI values.

In this project, a candidate reference device must produce profiles that cross correlate to the benchmark profile measurements with a score of 0.98 or better for IRI filter output. In the 2004 Round-up, a cross correlation of IRI filter output of at least 0.98 corresponded to a 95th percentile level of agreement in overall IRI of 1.5 percent or better. This rather tight tolerance was selected for two reasons. First, most profiler certification programs compare measurements from candidate profilers to only one reference profile measurement, since repeat reference measurements add expense to the process. When only one measurement is available, no opportunity exists for eliminating random errors in the summary index value. Second, a high level of cross correlation ensures that the details of the profile, and not just the summary index, are accurate. This is very important if a reference device is employed to verify production profilers that will locate isolated rough spots along the pavement or diagnose the source of excessive roughness.

A correlation level of 0.98 is also required for slope profile in the long and medium wavebands in anticipation of other roughness indices that are based on vehicle vertical vibration but emphasize a different portion of the waveband of interest. The requirement for the short waveband is relaxed somewhat to 0.94, because:

- Correlation in the short waveband is very sensitive to profiler footprint and low-pass filtering methods, and the most relevant methods for these aspects of profile measurement have not yet been established.
- Small errors in longitudinal distance measurement degrade correlation in the short waveband, even when the profiles under comparison are as short as 528 ft.

A correlation threshold of 0.98 for IRI filter output is very stringent. For example, only 184 profile pairs of profiles out of 445,669 from the 2004 Round-up achieved this level of agreement. However, the 2004 Round-up was one of the first major studies that applied cross correlation for rating of profile agreement. Hopefully, profiler manufacturers and operators will be able to improve their performance with greater familiarity with the rating system.

A more recent round-up at MnRoad in October, 2006 provided encouraging results. The MnRoad round-up featured six inclinometer-based “reference” profilers and two

inertial profilers on a transversely tined test section and an asphalt test section of tight mix. Appendix D briefly describes the experiment and provides summary results. A majority of the devices in this experiment achieved composite repeatability scores of 0.98 or better. In addition, many of the profilers correlated to each other with a composite score in the high 90s.

Phase Shift

The performance requirements for reference profiler repeatability and agreement to the benchmark profile measurement do not include explicit criteria for limiting phase shift. However, the stringent thresholds for cross correlation to the reference measurement constitute an implicit limitation on phase shift. This is because application of a filter with non-linear phase response to the candidate profile, but not to the benchmark profile, penalizes their correlation level. The penalty is caused by distortion of the profile that moves features from different parts of the waveband of interest an unequal amount. The longitudinal offset between profiles that provides the best will occur for part of the waveband (e.g., the part that contributes the most to the variance), but not all of it. The penalty usually grows in significance for broad-banded analysis, such as the IRI. Since the correlation threshold for a passing score is so high, even a small penalty may contribute significantly a failing score.

The penalty to cross correlation of IRI filter output after application of a 3rd order Butterworth filter demonstrates this effect. Figure C–1 shows the degradation in cross correlation on two profiles with idealized spectral content. The profiles were generated artificially to provide distinct combinations of Gaussian white noise slope, Gaussian white noise elevation, and Gaussian white noise spatial acceleration. The artificial roads featured in Figure C–1 include a profile of pure white noise slope, and white noise slope combined with white noise spatial acceleration.

The first example is a common simplification of road profile statistical properties. The second example corresponds to a “wavy” road, and is similar in spectral content to a proposed spectral model of European roads (LaBarre, 1970). Sayers (1986) proposed these examples are part of a representative set of surrogates for paved roads is studies of vehicle durability. The set included another example that is not shown in Figure C–1, because it yielded results so close to that of white noise slope. This was white noise slope combined with white noise elevation. A full description of the artificial roads appears in Karamihas (2005).

Figure C–1 examines the effect of pre-processing a profile with a 3rd order Butterworth high-pass filter of various cut-off wavelengths on cross correlation of IRI filer output. Each point in the figure represents the cross correlation of an IRI-filtered profile to a copy of itself, where the copy passed through the high-pass filter before application of the IRI filters. Each comparison covered nearly 10 miles of profile to allow the statistical properties of the artificial profile to converge to the desired spectral model. The calculations excluded some profile at the start and end of the profile to eliminate the influence of the initial transient caused by he filters.

For the white noise slope profile, the correlation level degrades to about 0.992 at a cut-off wavelength of 300 ft. For the wavy profile, the correlation degrades to 0.978. The penalty to correlation becomes even more serious for shorter cut-off wavelength values, because the waveband of interest is more strongly affected. This shows that application of a high-pass filter with a non-linear phase shift can very easily prevent a candidate reference profiler from obtaining a passing accuracy score.

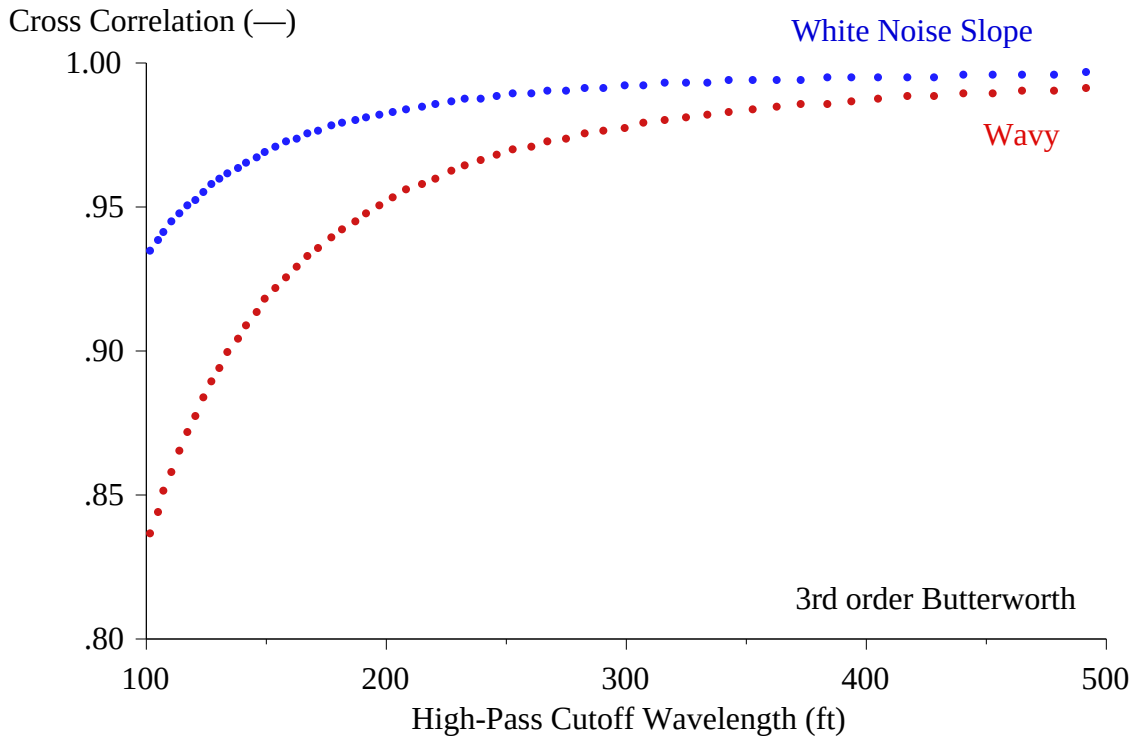

Figure C–1. Penalty to cross correlation caused by a Butterworth filter.

In practice, the test sections will be as short as 500 ft. Using a segment length of 500 ft would not permit the artificial profiles to converge to the desired idealized spectral shape, and a range of results is possible at each cut-off wavelength. For example, splitting the wavy road into 100 segments, each 528-ft long, produces correlation values from 0.972 to 0.999 at a cut-off wavelength of 300 ft.

Interpolation

Profilers of differing make or model rarely store profiles at the same interval. When two profiles are cross correlated, at least one of them must be re-sampled so that they will have the same recording interval. Karamihas (2004) recommend that the profile from the candidate device be re-sampled using interpolation to the recording interval of the reference device. When the original recording interval of the candidate profile is not an integer multiple of the recording interval of the reference profile, the interpolation smoothens the candidate profile. Unfortunately, reference profilers often record profile at greater interval than the candidate device under comparison. Further, many reference devices record profile at an interval that is too long for accurate measurement of IRI (Karamihas, 2005).

The smoothing that occurs during interpolation affects the correlation level between two profiles in a manner that does not have a systematic relationship to the most relevant aspects of their agreement. In a comparison of reference devices in common use that was conducted at MnRoad in October, 2006, interpolation affected cross correlation level by as much as 0.029. (See Appendix D.) (Note that the effect was significantly smaller when both profiles observed published standards for profile recording interval.) The effect was virtually eliminated by up-sampling both profiles to a common recording interval that was an integer factor of the recording interval from both devices under comparison. In this case, all of the devices recorded profile at an interval that was some multiple of 0.2 in (5.08 mm). However, when the final interval after up-sampling is sufficiently small, some smoothing can be tolerated. For example, up-sampling to an interval of 0.5 in (12.7 mm) provided results to within 0.00067 when compared to the analysis performed using 0.2 in (5.08 mm).

When candidate reference profiles are compared to benchmark profiles, both profiles will be up-sampled to either (1) an interval that divides into both recording interval values by an integer amount, or (2) a recording interval of 0.2 in (5.08 mm).

Longitudinal Distance Measurement

High cross correlation between profiles requires that both the roughness level and profile shape match over the entire length under comparison. As a result, errors in longitudinal distance measurement (known as “DMI errors”) reduce cross correlation level. This occurs even if the profiles agree perfectly with the exception of DMI error. This is because peaks and troughs within the profile can no longer line up over the entire length of profile. The penalty to cross correlation caused by DMI error depends on the error level, the profile length, and the waveband under examination.

For example, DMI error of just 0.1 percent causes misalignment of a 1-ft long sine wave by half of its length over each 500 ft of distance. Misaligned as such, the troughs appear in the locations where the peaks should appear. This would greatly reduce the correlation under comparison to a profile with no longitudinal distance measurement error.

Figure C–2 shows the penalty to cross correlation of IRI filter output caused by DMI error on a 500-ft long asphalt test section (Cell 31) and a 500-ft long concrete test section (Cell 39) at MnRoad. The subject profiles were measured by an inclinometer-based profiler, recorded at an interval of 1 in and, up-sampled to an interval of 0.2 in. The figure shows the cross correlation level of an unmodified profile to that of a profile with the recording interval altered to simulate a given DMI error level. On the asphalt section, DMI error of 0.1 percent reduces the correlation to about 0.995. Correlation reduces to about 0.997 on the concrete section. Although DMI error alone is not enough to carry the cross correlation below the threshold value of 0.98, the penalty should motivate an effort to avoid excessive DMI error.

Figure C–3 shows the same analysis for the short waveband. When cross correlating in the short waveband, even very small DMI error causes a critical penalty to the agreement level. This is corrected by using shorter sections for comparison in the short waveband. Figure C–4 provides an example. Profiles are again correlated in the short waveband, but

only over 105.6 ft (32.2 m). Cross correlation in the short waveband will be limited to segments of this length.

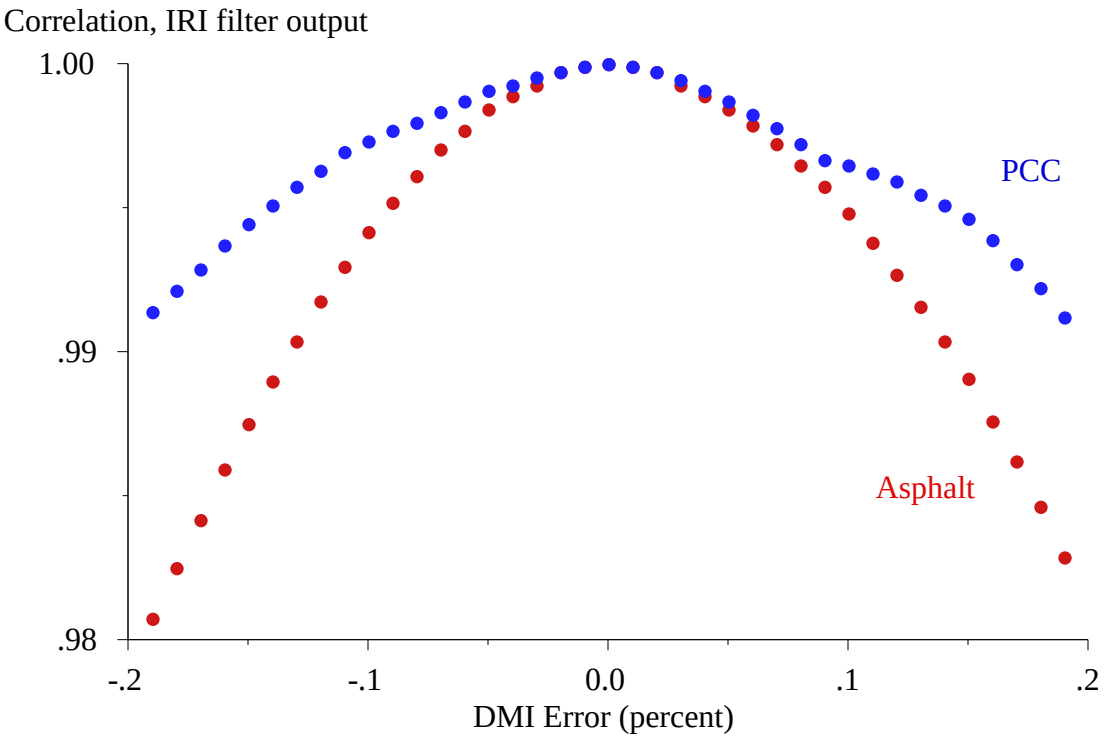

Figure C–2: Influence of DMI error on the IRI waveband.

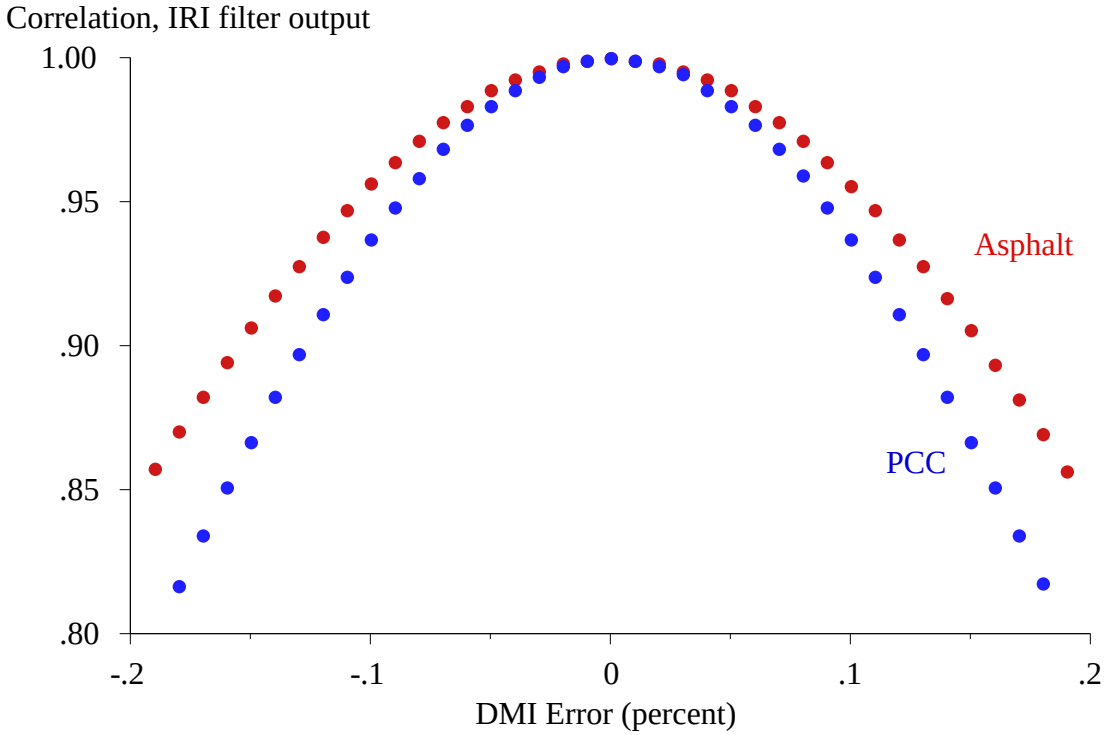

Figure C–3: Influence of DMI error on the short waveband.

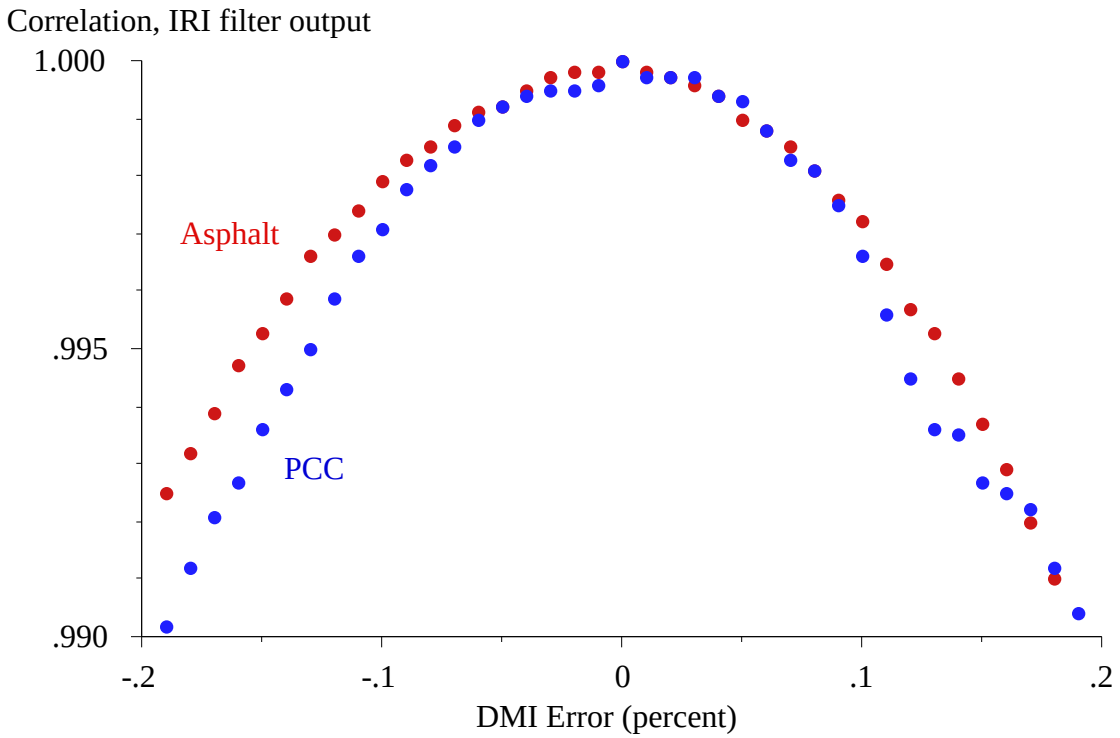

Figure C–4: Influence of DMI error on the short waveband, short sections.

Appendix D: 2004 FHWA Round-up Results

The purpose of this appendix is to examine the relationship between error in overall IRI value and the cross correlation level between profiles. When this relationship is defined, it may be used to set cross correlation thresholds for repeatability and agreement to a reference measurement. To help establish this relationship, all possible comparisons of individual measurements from the 2004 FHWA Profiler Round-up were examined as individual samples. To do this, any pair of profiles that covered the same wheel track on the same segment of road was cross correlated using IRI filter output. The level of cross correlation was then "paired" with the percent difference in IRI.

Figure D–1 shows the absolute IRI error level versus cross correlation for pairs of repeat measurements. These are any pairs of two measurements of the same road segment by the same profiler. The plot covers a range of error level up to 40 percent and cross correlation level above 0.50. This range includes 4,574 or the 5,219 possible repeatability comparisons. (The others are out of the range of the plot.)

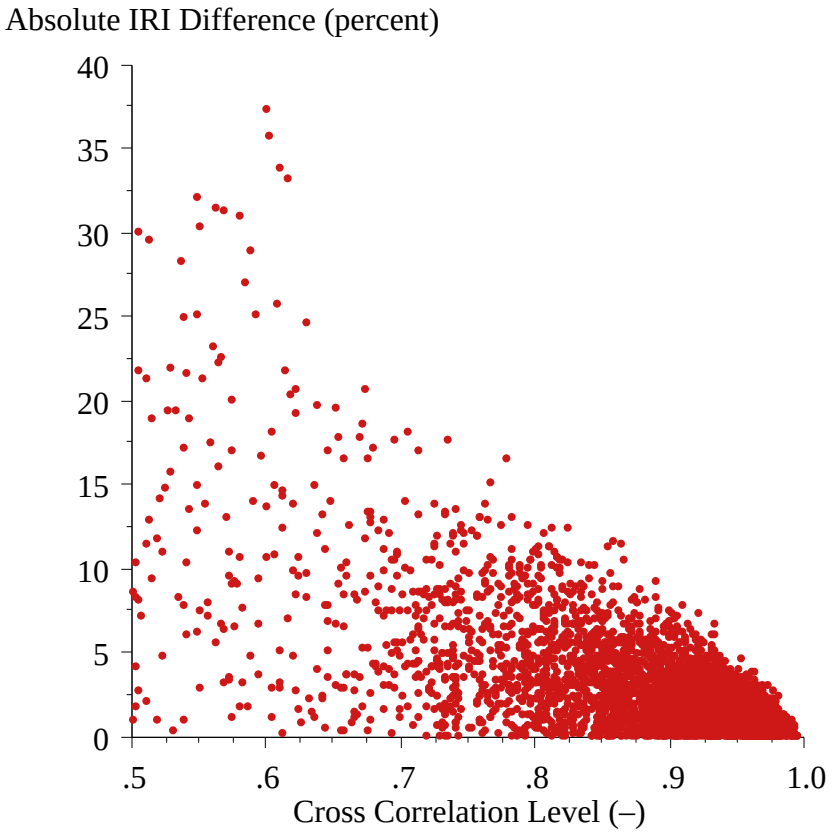

Figure D–1. Comparison of absolute IRI error and cross correlation level.

Figure D–1 shows that each correlation level is associated with a maximum error level in IRI, and that the maximum expected error level in IRI decreases as correlation improves. It is this aspect of the relationship between IRI error and cross correlation that will be used

to establish correlation thresholds. Note also that it is possible to have a very low error in IRI, even when the cross correlation is low. In these cases, the overall IRI agreed, even though the details of the profile did not. This is not desirable, because it is likely that the profiler would not perform well consistently in the field. Further, the details of the profile are often needed for more detailed study of the pavement surface, such detection on localized roughness.

The calculation of IRI error and cross correlation level for all possible combinations within the round-up resulted in 445,669 pairs of values. These pairs include comparisons across different types of profiler (inclinometer-based and inertial, high-speed inertial and lightweight inertial, etc.), inertial profilers with their own repeat measurements, comparisons across different inertial profilers, and comparisons across different slow-speed devices. For example, 275 profiles of section 1 were included in the study. This permitted 74,704 comparisons. Note that each comparison of two measurements from unique devices were made twice, so that one of the profiles could take the role of reference measurement in each comparison. This was needed because the process does not have reciprocity.

Once the level of IRI error and cross correlation was computed for all pairs, they were assembled into bins by their cross correlation level. Each bin covered a range of 0.01 (out of 1) along the scale. For example, the bin that ranged from 0.92 to 0.93 included 5,601 pairs. The distribution of IRI error level within this bin is shown in Figure D–2.

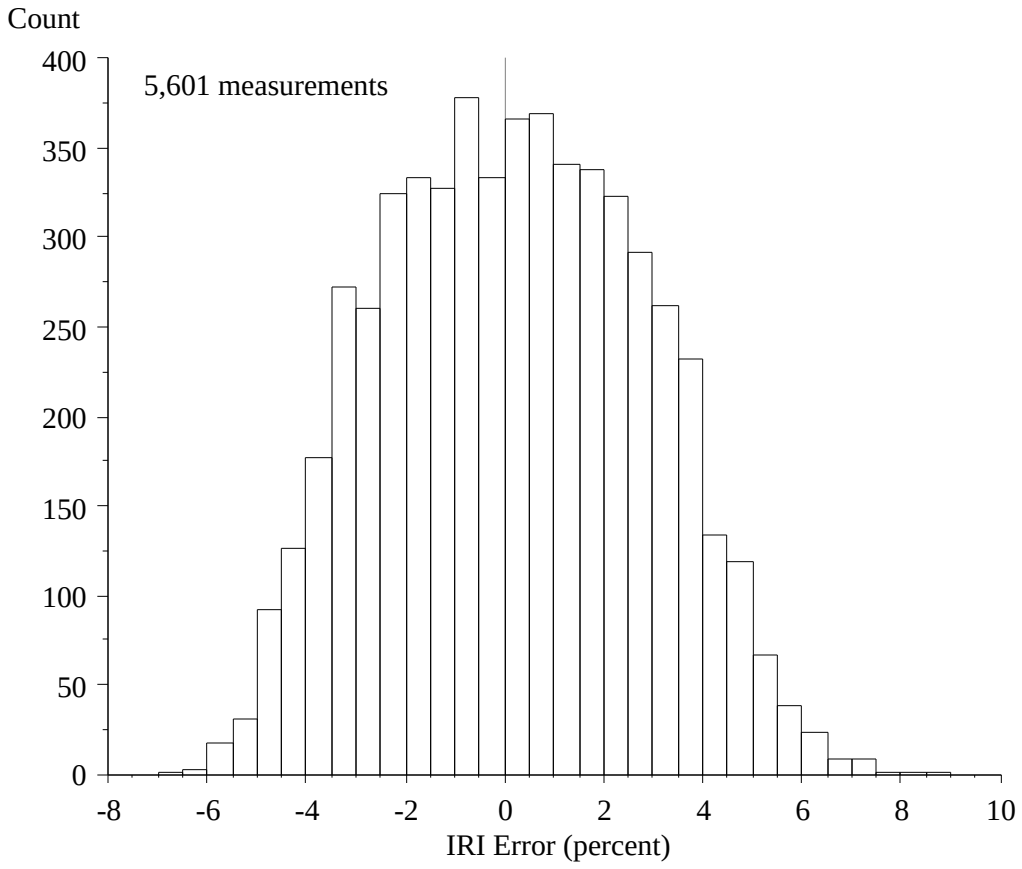

Figure D–2. Distribution of IRI disagreement, cross correlation 0.92-0.93.

The content of this distribution can be summarized in five ways:

1. **Average**: The average value of IRI error. This should be small, but it will always be greater than zero. (Consider a pair of IRI measurements of 1.00 m/km and 1.05 m/km. They will yield two values of error: 5 percent and -4.76 percent. This non-linearity will cause the average error level to have a non-zero value.)
2. **RMS**: The root mean square error level includes the influence of upward and downward errors. When it is considered in conjunction with the average error level, it would be enough to define the distribution if the Gaussian assumption was reasonable. In Figure D–1, this is not the case.
3. **95th Percentile**: The 95th percentile error level includes the influence of upward and downward errors also. A desired expected 95th percentile error level in IRI should be used to set a minimum cross correlation level between profiles.
4. **Maximum Error**: This is the maximum level of IRI upward bias error observed within the range of cross correlation level under examination. It is simply included to place a bound on the possible error level, and warn users of these results of the inevitable anecdote that a measurement with a high level of cross correlation still showed some disagreement in IRI.
5. **Minimum Error**: This is the maximum level of IRI downward bias error observed within the range of cross correlation level of under examination.

These five quantities are displayed in Figure D–3 for a broad range of bins from 0.20 through 1.00. In the figure, the set of values for each bin is provided at its center. (For example, the values for the bin from 0.92 though 0.93 are provided at a cross correlation value of 0.925.) The values displayed in Figure D–3 are also listed in Table D–1, below, so that individual values of interest are easier to read. The table also lists the number of pairs within each bin. The error levels grow quite high when the cross correlation level decreases below about 0.80. The figure is therefore repeated for values of cross correlation above 0.75 in Figure D–4.

Figure D–4 shows a clear relationship between the cross correlation level and the 95th percentile error level expected in IRI measurement. The following thresholds are proposed for various “classes” of profiler:

- **Reference Class**: At a cross correlation level of 0.97, you may expect your overall IRI measurements to agree within 2 percent of each other 95 percent of the time.
- **Project Class**: At a cross correlation level of 0.92, you may expect your overall IRI measurements to agree within 5 percent of each other 95 percent of the time.
- **Network Class**: At a cross correlation level of 0.81, you may expect your overall IRI measurements to agree within 10 percent of each other 95 percent of the time.

Further, a value of 0.92 could also be used to establish a threshold for construction quality control.

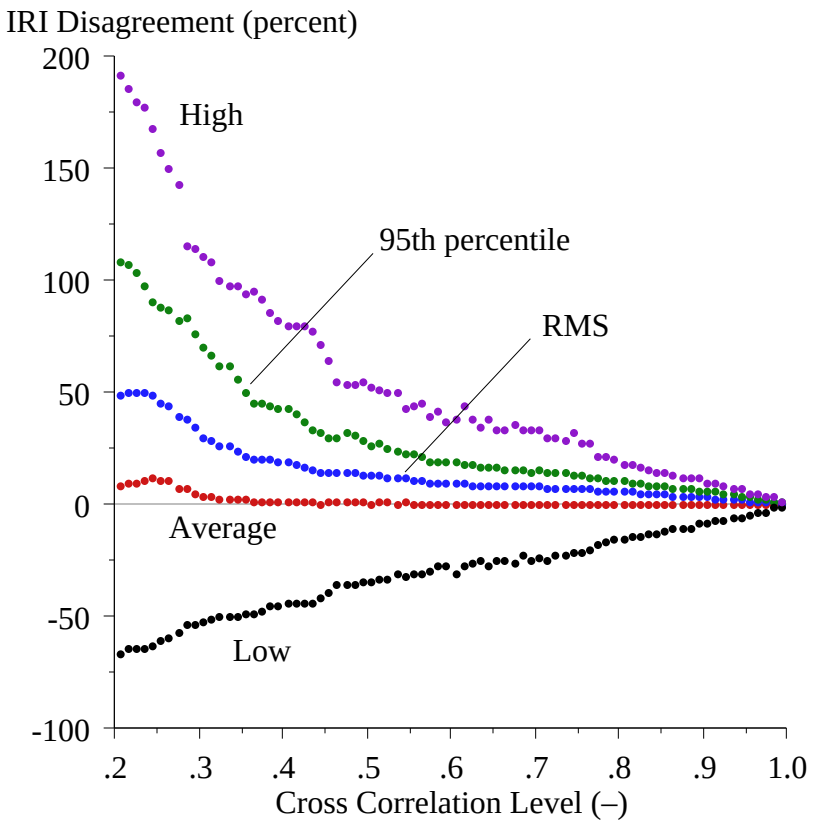

Figure D–3. IRI disagreement at various cross correlation levels.

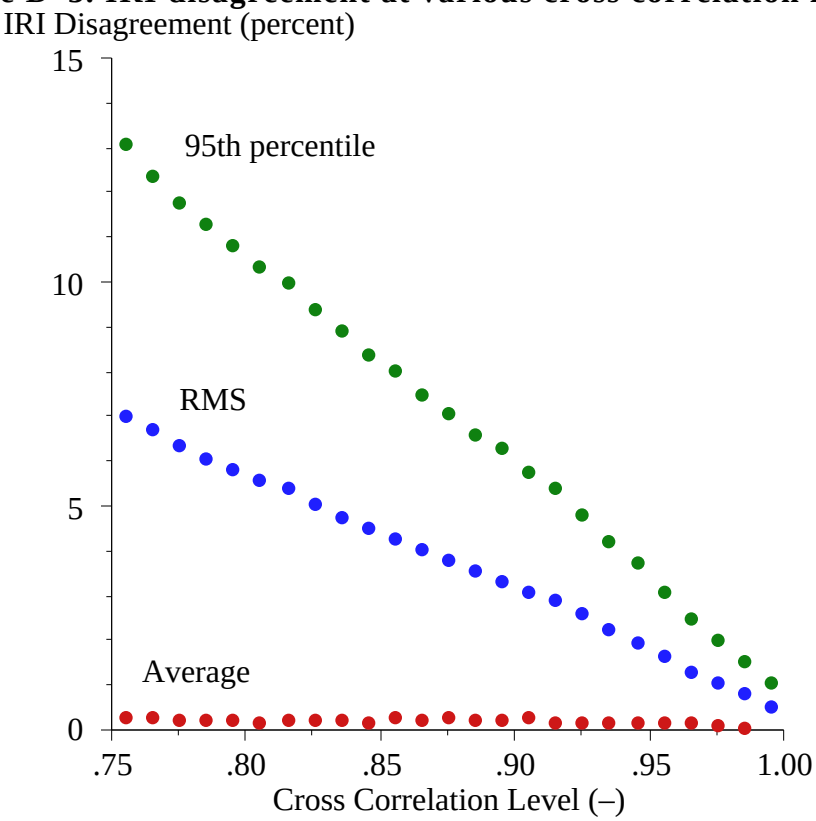

Figure D–4. IRI disagreement at high cross correlation levels.

Table D–1. Expected IRI error associated with cross correlation level.

Cross Correlation Range		Number of Comparisons	Error Level in IRI Measurement (Percent)				
From	To		Average	RMS	95th Percentile	Low	High
0.99	1.00	13	-0.15	0.52	1.07	-1.07	0.81
0.98	0.99	171	0.04	0.83	1.54	-1.38	3.42
0.97	0.98	849	0.10	1.04	2.00	-3.49	3.79
0.96	0.97	2054	0.16	1.31	2.48	-4.16	4.81
0.95	0.96	3095	0.20	1.64	3.12	-4.87	5.21
0.94	0.95	3963	0.18	1.96	3.73	-5.78	6.84
0.93	0.94	4965	0.18	2.26	4.23	-6.22	6.82
0.92	0.93	5601	0.18	2.62	4.80	-6.62	8.92
0.91	0.92	6398	0.20	2.93	5.43	-7.65	9.12
0.90	0.91	7096	0.27	3.11	5.76	-8.11	9.57
0.89	0.90	7490	0.24	3.33	6.30	-8.71	11.72
0.88	0.89	8028	0.23	3.56	6.63	-10.77	11.82
0.87	0.88	8432	0.29	3.80	7.10	-10.38	12.23
0.86	0.87	8485	0.21	4.04	7.50	-10.97	13.36
0.85	0.86	8754	0.27	4.29	8.05	-11.48	14.76
0.84	0.85	9123	0.19	4.53	8.41	-12.97	14.73
0.83	0.84	8988	0.23	4.76	8.92	-12.99	15.99
0.82	0.83	8809	0.27	5.08	9.42	-14.22	16.69
0.81	0.82	8691	0.21	5.40	10.00	-14.45	17.62
0.80	0.81	8742	0.19	5.62	10.37	-15.24	18.15
0.79	0.80	8455	0.22	5.82	10.82	-15.40	20.72
0.78	0.79	8252	0.26	6.10	11.31	-16.79	21.57
0.77	0.78	8164	0.26	6.39	11.80	-17.28	21.99
0.76	0.77	8236	0.30	6.73	12.39	-20.29	26.90
0.75	0.76	8006	0.30	7.02	13.10	-21.62	27.19
0.74	0.75	7837	0.28	7.29	13.61	-20.90	32.35
0.73	0.74	7836	0.29	7.42	14.04	-22.75	29.15
0.72	0.73	7667	0.34	7.62	14.50	-23.00	29.59
0.71	0.72	7407	0.30	7.64	14.53	-24.54	30.33
0.70	0.71	6927	0.18	7.87	15.17	-24.31	33.00
0.69	0.70	6964	0.29	7.78	14.81	-24.85	32.90
0.68	0.69	6758	0.24	7.86	15.03	-22.89	33.71
0.67	0.68	6565	0.18	8.12	15.76	-26.29	35.72
0.66	0.67	6333	0.30	8.28	15.90	-24.77	32.93
0.65	0.66	6170	0.33	8.49	16.65	-25.47	33.46
0.64	0.65	5966	0.14	8.71	16.74	-27.42	37.51
0.63	0.64	5866	0.45	8.82	17.26	-24.62	34.22
0.62	0.63	5731	0.42	8.87	17.33	-25.99	38.45
0.61	0.62	5593	0.35	9.28	18.12	-27.91	43.65
0.60	0.61	5455	0.47	9.53	18.63	-30.60	37.50
0.59	0.60	5075	0.40	9.87	19.61	-27.10	37.34
0.58	0.59	4879	0.34	9.76	19.44	-27.36	41.80
0.57	0.58	4768	0.41	9.89	19.12	-29.50	38.70
0.56	0.57	4584	0.48	10.53	20.94	-31.27	45.45
0.55	0.56	4285	0.58	10.94	22.35	-30.78	43.66

162,141 comparisons are excluded, because their cross correlation levels are outside the limits of the table.

Appendix E: 2006 MnRoad Round-up

This appendix provides summary results from analysis of profiler comparison data collected at MnRoad on October 16-18, 2006. The experiment compared several inclinometer-based "reference" profilers on two test sections. For a complete report of this experiment and its results, see Perera (2006):

The experiment covered two test sections: (1) a hot mix asphalt section (Cell 31) and (2) a transversely tined Portland cement concrete (PCC) section (Cell 39). Each test section included a very clear yellow strip of paint along the track of interest. Six inclinometer-based devices participated in the experiment, listed in Table E–1 below. An Ames Engineering lightweight also measured each section five times using a guide to maintain a consistent lane position. This device included two profilers mounted in series on the same host vehicle, about 1.5 ft apart. One profiler used TriODS height sensors and the other used a RoLine laser height sensor. Both profilers recorded data at an interval of 0.1 ft.

All the measurements occurred on October 17, 2006, with the exception of the Dipstick runs, which took place the day before and the day after. Several participants mentioned the cold, wet and windy weather.

Table E–1. Inclinometer-based profilers.

Device	Operator	Repeats per Section	Recording Interval (in)
ARRB Walking Profiler	Minnesota DOT	3	9.5
SSI Walking Profiler	SSI	3	1
SurPro 2000	Wisconsin DOT	3	1
SurPro 2000, SN 36	ICC	3	1
SurPro 2000, wide wheels	ICC	3	1
Face Model 2200 Dipstick, SN 43015	EBA	2	12

International Roughness Index

Table E–2 and E–3 provide International Roughness Index (IRI) values for each test run. On the asphalt section (Cell 31), the calculations cover the first 500 ft of profile. On the PCC section (Cell 39), the calculations cover the first 532 ft. In some cases, the profiles were slightly shorter than the set distance. For the Ames lightweight measurements with the RoLine sensor, the starting and ending points for IRI calculations were shifted 1.5 ft downstream to make up for the profiler mounting offset.

In the IRI calculations, the moving average was applied to data from both Ames lightweight profilers and the SSI Walking Profiler. The moving average was not applied to the Dipstick or ARRB Walking Profiler data, because of the long sample interval. The moving average was not applied to any of the SurPro 2000 data, because the geometric configuration of the device amounts to an equivalent effect. (Inspection of the PSD plots verifies the mechanical filtering.) When performing the IRI filtering for cross correlation analysis, the moving average was also applied (or not) as described previously.

Table E–2. Asphalt section IRI values (in/mi).

Device	Run 1	Run 2	Run 3	Run 4	Run 5
ARRB WP	87.6	86.6	88.8		
Dipstick	85.9	85.7			
SP 2000 (SN 36)	90.5	89.5	90.1		
SP 2000 (Wide)	88.6	89.6	89.3		
SP 2000 (Wisc)	89.7	90.4	91.6		
SSI WP	87.2	88.1	87.5		
Ames TriODs	90.5	89.4	89.6	89.5	89.1
Ames RoLine	88.9	88.2	88.2	88.2	88.0

Table E–3. PCC section IRI values (in/mi).

Device	Run 1	Run 2	Run 3	Run 4	Run 5
ARRB WP	76.1	75.6	75.8		
Dipstick	75.0	75.5			
SP 2000 (SN 36)	77.6	77.8	78.6		
SP 2000 (Wide)	76.9	77.1	77.7		
SP 2000 (Wisc)	78.0	77.5	78.9		
SSI WP	74.8	78.3	76.6		
Ames TriODs	77.0	77.4	78.0	78.4	78.6
Ames RoLine	76.2	76.2	76.9	76.7	76.5

Cross Correlation

Table E–4 and E–5 provide the results of cross correlation analysis. Profiles were only correlated after application of the filters within the IRI algorithm. This included conversion to slope, application of a moving average (if needed), and application of a Golden car simulation of suspension stoke.

In each comparison, one profile served as the correlation reference, and the"correlated" profile was interpolated to the same sample interval as the correlation reference. Note that the interpolation was performed after the filtering. When the profiles under comparison do not have the same sample interval, the results may depend on which profile is selected as the reference. (The results below show that this effect was limited to 0.02 on the correlation scale for this data set.)

Each correlation value was generated by cropping 6.6 ft (2 m) of the start and end of the reference profile, then shifting the correlated profile ±6.6 ft to find the offset that provided the best match. The optimal offset was usually small, since rolling and walking devices are able to trigger at a set starting point fairly accurately. Note that the profiles from the device with the RoLine height sensor were offset about 1.5 ft from the others, since it was mounted roughly 1.5 ft behind the TriODS system, but triggered at the same time.

Each of the table entries provided above is the average of several individual cross correlation values. For example, when data from a profiler that made five repeat measurements were compared to those of a profiler that made three repeat measurements, the corresponding table entry is the average of all fifteen comparisons.

Table E–4. Asphalt section, average cross correlation values.

		Correlated Device							
	"Ref." Device	1	2	3	4	5	6	7	8
1	ARRB WP	0.94	0.90	0.91	0.92	0.89	0.78	0.91	0.93
2	Dipstick	0.89	0.96	0.92	0.92	0.90	0.84	0.91	0.93
3	SP 2000 (SN 36)	0.92	0.94	0.99	0.99	0.98	0.89	0.98	0.98
4	SP 2000 (Wide)	0.93	0.93	0.99	0.99	0.97	0.88	0.98	0.98
5	SP 2000 (Wisc)	0.90	0.89	0.98	0.97	0.98	0.89	0.96	0.96
6	SSI WP	0.78	0.87	0.89	0.89	0.89	0.90	0.87	0.87
7	Ames TriODs	0.93	0.90	0.98	0.98	0.97	0.87	0.98	0.98
8	Ames RoLine	0.93	0.93	0.98	0.98	0.96	0.87	0.98	0.99

Table E–5. PCC section, average cross correlation values.

		Correlated Device							
	"Ref." Device	1	2	3	4	5	6	7	8
1	ARRB WP	0.97	0.94	0.94	0.95	0.94	0.78	0.94	0.96
2	Dipstick	0.94	0.95	0.94	0.95	0.94	0.83	0.94	0.96
3	SP 2000 (SN 36)	0.94	0.94	0.99	0.98	0.99	0.83	0.97	0.97
4	SP 2000 (Wide)	0.95	0.95	0.98	0.98	0.98	0.83	0.97	0.98
5	SP 2000 (Wisc)	0.94	0.95	0.99	0.98	0.98	0.84	0.97	0.97
6	SSI WP	0.78	0.84	0.83	0.83	0.84	0.85	0.82	0.83
7	Ames TriODs	0.94	0.94	0.97	0.97	0.97	0.82	0.97	0.97
8	Ames RoLine	0.96	0.96	0.97	0.98	0.97	0.83	0.97	0.99

The lack of reciprocity in the results above is an artifact of the calculation procedure. The smoothing that takes place when one profile is re-sampled to the recording interval of another causes this effect, but only when the original recording interval is not an integer multiple of the new recording interval.

To reduce the smoothing effect, the analysis was repeated after up-sampling all of the profiles to a recording interval of 0.2 in (5.08 mm). Table E–6 and E–7 show the change in average cross correlation value. The largest change was 0.029, and the only significant changes occurred when either the Dipstick or ARRB WP were involved in the comparison. This is because they both recorded profile at a larger interval. The up-sampling did not significantly affect the composite correlation levels among the devices that recorded profile at an interval of 1 in (25.4 mm) or less.

It will not always be possible to find a new recording interval that divides evenly into the recording interval of every profiler under comparison. However, up-sampling to a sufficiently small recording interval is expected to greatly reduce the smoothing effect in the waveband of interest. For example, up-sampling to an interval of 0.5 in (12.7 mm) instead of 0.2 in (5.08 mm) did not change any of the composite correlation levels by more than 0.0004, and it did not change any individual comparisons by more than 0.00067.

Table E–6. Asphalt section, cross correlation change with up-sampling.

		Correlated Device							
	"Ref." Device	1	2	3	4	5	6	7	8
1	ARRB WP	.003	.015	.005	.006	.007	.002	.006	.006
2	Dipstick	.029	.000	.014	.014	.014	.015	.013	.014
3	SP 2000 (SN 36)	.001	-.005	.000	.000	.000	.000	.000	-.001
4	SP 2000 (Wide)	-.011	.007	.000	.000	.000	.000	.001	.000
5	SP 2000 (Wisc)	-.012	.024	.000	.000	.000	.001	-.001	.000
6	SSI WP	-.005	-.008	.000	.000	.000	.000	.000	.000
7	Ames TriODs	-.005	.021	.000	.000	.000	.000	.000	.000
8	Ames RoLine	.009	.008	.000	.000	.000	.000	.000	.000

Table E–7. PCC section, cross correlation change with up-sampling.

		Correlated Device							
	"Ref." Device	1	2	3	4	5	6	7	8
1	ARRB WP	.000	.010	.000	.000	-.001	-.002	.000	.000
2	Dipstick	.012	.016	.007	.007	.007	.002	.007	.007
3	SP 2000 (SN 36)	-.002	.002	.000	.000	.000	.000	.000	.000
4	SP 2000 (Wide)	-.004	.000	.000	.000	.000	.000	.000	.000
5	SP 2000 (Wisc)	-.005	-.001	.000	.000	.000	.000	.000	.000
6	SSI WP	-.001	.003	.000	.000	.000	.000	.000	.000
7	Ames TriODs	-.004	.001	.000	.000	.000	.000	.000	.000
8	Ames RoLine	.002	.001	.000	.000	.000	.000	.000	.000

Appendix F: Butterworth Filters

The Butterworth filter set provided for ProVAL includes a high-pass filter and a low-pass filter. The band-pass filtering option simply applies the high-pass filter with the requested long-wavelength cut-off then the low-pass filter with the requested short wavelength cut-off. Both filters are applied in a cascaded form of a third order Butterworth filter in the forward and reverse directions. This raises the order of each filter to six.

Both filters will use double precision 8-byte floating point.

Low-Pass Filter

A third order Butterworth low-pass filter has the transfer function:

$$H(s) = \frac{1}{s^3 + 2s^2 + 2s + 1}$$

The filter may be cascaded by applying a first order Butterworth filter:

$$H_1(s) = \frac{1}{s + 1}$$

and a complementary second order filter:

$$H_2(s) = \frac{1}{s^2 + s + 1}$$

Although the two versions of the filter have the same transfer function, the cascaded version is more stable numerically than the un-cascaded version. The cascaded version of the filter was applied to all the profiles from the 2004 FHWA profiler round-up. Spectral analysis on the raw and filtered profiles produced numerical transfer functions for all profiles that closely approximated the desired theoretical transfer function.

The filters described above produce a phase lag in the conditioned profile. This was eliminated by applying both the first order and second order filters twice: once in the forward direction and once in the reverse direction. Note that this raises the overall order of the filter to six. This also changes the interpretation of the cut-off wavelength. If the first order and second order filters are applied using a given cut-off wavelength L, the 3dB gain reduction will occur at that wavelength. However, when they are applied again, the reduction at that wavelength will be larger. To get the appropriate gain reduction at a desired wavelength L', the value of L must be adjusted as follows:

$$L = (\sqrt{2} - 1)^{(1/6)} \bullet L'$$

The minimum value oSn2

f L' is restricted as follows:

$$L'_{min} = 2 \bullet \Delta x \bullet (\sqrt{2} - 1)^{(-1/6)}$$

This is done because the filter was found to be numerically unstable for lower values of L'.

The output of each filter includes an initial transient. This is most evident when the filter is applied to profiles with a significant slope at the leading end. However, the severity of the initial transient depends on the sequence of the filter components. The filters are applied in the following sequence:

Step 1: first order, forward direction

Step 2: second order, reverse direction

Step 3: first order, reverse direction

Step 4: second order, forward direction

This sequence virtually eliminated the transient at the end of the profile caused by the reverse-direction filters. It also reduced the transient at the start of the profile as much or more than any other possible sequence, and much more than the un-cascaded version of the third order Butterworth filter.

Step 1: First Order, Forward Direction

For a given input profile (P), the first order filter applied in the forward direction produces the output (F_1) as follows:

$$F_1(i) = \frac{1}{D_{10}}(N_{10}P(i) + N_{11}P(i-1) - D_{11}F_1(i-1)) \qquad \text{(F–1)}$$

Where P and F_1 are stored as sequential arrays with index values that begin at 1 and increase to N_S along the profile. Equation F–1 is applied by stepping the index value (i) through the range from 2 to N_S. The first point in the filtered profile can not be calculated using equation F–1, since it would require values that are out of range of the input profile. Instead, F_1 is initialized by assigning the first point in it to the value of the first point in P.

$$F_1(1) = P(1) \qquad \text{(F–2)}$$

The symbols D and N in equation F–1 are filter coefficients:

$$N_{10} = N_{11} = 1,\ D_{10} = 1 + c, \text{ and } D_{11} = 1 - c \qquad \text{(F–3)}$$

These coefficients depend on the profile recording interval (Δx) and cut-off wavelength (L) through the value of c:

$$c = \cot(\pi \bullet \Delta x/L) \qquad \text{(F–4)}$$

Step 2: Second Order, Reverse Direction

The second order (complement) reverse filter transforms F_1 to the intermediate signal F_2 as follows:

$$F_2(i) = \frac{1}{D_{20}}(N_{20}F_1(i) + N_{21}F_1(i+1) + N_{22}F_1(i+2) - D_{21}F_2(i+1) - D_{22}F_2(i+2)) \qquad \text{(F–5)}$$

Where F_1 and F_2 are stored as sequential arrays with index values that begin at 1 and increase to N_S along the profile. Equation F–5 is applied by stepping the index value (i) through the range in reverse from $N_S - 2$ to 1. The filter coefficients are:

$$N_{20} = N_{22} = 1,\ N_{21} = 2,$$

$$D_{20} = 1 + c + c^2,$$

$$D_{21} = 2 - 2c^2, \text{ and}$$

$$D_{22} = 1 - c + c^2 \qquad \text{(F–6)}$$

The value of c is calculated as shown in equation F–4.

The last two points in the intermediate signal (F_2) can not be calculated using equation F–5, since it would require values that are out of range of the signal F_1. Instead, F_2 is initialized by assigning the last point in it to the value of the last point in F_1.

$$F_2(N_S) = F_1(N_S) \qquad \text{(F–7)}$$

The second to last point in F_2 is calculated using the equations for a first-order filter applied in the reverse direction:

$$F_2(N_S - 1) = \frac{1}{D_{10}}(N_{10}F_1(N_S - 1) + N_{11}F_1(N_S) - D_{11}F_2(N_S))$$

or

$$F_2(N_S - 1) = \frac{1}{D_{10}}(N_{10}F_1(N_S - 1) + (N_{11} - D_{11})F_1(N_S)) \qquad \text{(F–8)}$$

Where the coefficients D and N are defined by equation F–3. Note that equations F–7 and F–8 must be applied before equation F–5.

Step 3: First Order, Reverse Direction

The first order reverse filter transforms F_2 to the intermediate signal F_3 as follows:

$$F_3(i) = \frac{1}{D_{10}}(N_{10}F_2(i) + N_{11}F_2(i+1) - D_{11}F_3(i+1)) \qquad \text{(F–9)}$$

Where F_2 and F_3 are stored as sequential arrays with index values that begin at 1 and increase to N_S along the profile. Equation F–9 is applied by stepping the index value (i) through the range in reverse from $N_S - 1$ to 1. The filter coefficients are defined by equation F–3, above.

The last point in the intermediate signal (F_3) can not be calculated using equation F–9, since it would require values that are out of range of the signal F_2. Instead, F_3 is initialized by assigning the last point in it to the value of the last point in F_2.

$$F_3(N_S) = F_2(N_S) \qquad \text{(F–10)}$$

Note that equation F–10 must be applied before equation F–9.

Step 4: Second Order, Forward Direction

The second order (complement) filter transforms F_3 to the final signal F_4 as follows:

$$F_4(i) = \frac{1}{D_{20}}(N_{20}F_3(i) + N_{21}F_3(i-1) + N_{22}F_3(i-2) - D_{21}F_4(i-1) - D_{22}F_4(i-2)) \quad \text{(F–11)}$$

Where F_3 and F_4 are stored as sequential arrays with index values that begin at 1 and increase to N_S along the profile. Equation F–11 is applied by stepping the index value (i) through the range from 3 to N_S. The filter coefficients are defined in equation F–6, above.

The first two points in the filtered profile (F_4) can not be calculated using equation F–11, since it would require values that are out of range of the signal F_3. Instead, F_4 is initialized by assigning the first point in it to the value of the first point in F_3.

$$F_4(1) = F_3(1) \quad \text{(F–12)}$$

The second point in F_4 is calculated using the equations for a first-order filter:

$$F_4(2) = \frac{1}{D_{10}}(N_{10}F_3(2) + N_{11}F_3(1) - D_{11}F_4(1))$$

or

$$F_4(2) = \frac{1}{D_{10}}(N_{10}F_3(2) + (N_{11} - D_{11})F_3(1)) \quad \text{(F–13)}$$

Where the coefficients D and N are defined by equation F–3. Note that equations F–12 and F–13 must be applied before equation F–11.

High-Pass Filter

A third order Butterworth high-pass filter has the transfer function:

$$H(s) = \frac{s^3}{s^3 + 2s^2 + 2s + 1}$$

The filter may be cascaded by applying a first order Butterworth filter:

$$H_1(s) = \frac{s}{s+1}$$

and a complementary second order filter:

$$H_2(s) = \frac{s^2}{s^2 + s + 1}$$

Although the two versions of the filter have the same transfer function, the cascaded version is more stable numerically than the un-cascaded version. The cascaded version of the filter was applied to all the profiles from the 2004 FHWA profiler round-up. Spectral analysis on the raw and filtered profiles produced numerical transfer functions for all profiles that closely approximated the desired theoretical transfer function.

The filters described above produce a phase lag in the conditioned profile. This was eliminated by applying both the first order and second order filters twice: once in the forward direction and once in the reverse direction. Note that this raises the overall order of the filter to six. This also changes the interpretation of the cut-off wavelength. If the first order and second order filters are applied using a given cut-off wavelength L, the 3dB gain reduction will occur at that wavelength. However, when they are applied again, the reduction at that wavelength will be larger. To get the appropriate gain reduction at a desired wavelength L', the value of L must be adjusted as follows:

$$L = (\sqrt{2} - 1)^{(-1/6)} \bullet L'$$

The minimum value of L' is restricted as follows:

$$L'_{min} = 2 \bullet \Delta x \bullet (\sqrt{2} - 1)^{(-1/6)}$$

This is done because the filter was found to be numerically unstable for lower values of L'.

The output of each filter includes an initial transient. This is most evident when the filter is applied to profiles with a significant slope at the leading end. However, the severity of the initial transient depends on the sequence of the filter components. The filters are applied in the following sequence:

Step 1: first order, forward direction

Step 2: second order, reverse direction

Step 3: first order, reverse direction

Step 4: second order, forward direction

This sequence virtually eliminated the transient at the end of the profile caused by the reverse-direction filters. It also reduced the transient at the start of the profile as much or more than any other possible sequence, and much more than the un-cascaded version of the third order Butterworth filter.

Step 1: First Order, Forward Direction

For a given input profile (P), the first order filter applied in the forward direction produces the output (F_1) as follows:

$$F_1(i) = \frac{1}{D_{10}} (N_{10}P(i) + N_{11}P(i-1) - D_{11}F_1(i-1)) \qquad \text{(F–14)}$$

Where P and F_1 are stored as sequential arrays with index values that begin at 1 and increase to N_S along the profile. Equation F–14 is applied by stepping the index value (i) through the range from 2 to N_S. The first point in the filtered profile can not be calculated using equation F–14, since it would require values that are out of range of the input profile. Instead, F_1 is initialized by assigning the first point in it to zero.

$$F_1(1) = 0 \qquad \text{(F–15)}$$

The symbols D and N in equation F–14 are filter coefficients:

$$N_{10} = c,\ N_{11} = -c,\ D_{10} = 1 + c, \text{ and } D_{11} = 1 - c \qquad \text{(F–16)}$$

These coefficients depend on the profile recording interval (Δx) and cut-off wavelength (L) through the value of c:

$$c = \cot(\pi \bullet \Delta x/L) \qquad \text{(F–17)}$$

Step 2: Second Order, Reverse Direction

The second order (complement) reverse filter transforms F_1 to the intermediate signal F_2 as follows:

$$F_2(i) = \frac{1}{D_{20}}(N_{20}F_1(i) + N_{21}F_1(i+1) + N_{22}F_1(i+2) - D_{21}F_2(i+1) - D_{22}F_2(i+2)) \qquad \text{(F–18)}$$

Where F_1 and F_2 are stored as sequential arrays with index values that begin at 1 and increase to N_S along the profile. Equation F–18 is applied by stepping the index value (i) through the range in reverse from $N_S - 2$ to 1. The filter coefficients are:

$N_{20} = N_{22} = c^2,\ N_{21} = 2c^2,$

$D_{20} = 1 + c + c^2,$

$D_{21} = 2 - 2c^2,$ and

$D_{22} = 1 - c + c^2$ (F–19)

The value of c is calculated as shown in equation F–17.

The last two points in the intermediate signal (F_2) can not be calculated using equation F–18, since it would require values that are out of range of the signal F_1. Instead, F_2 is initialized by assigning the last point in it to zero.

$$F_2(N_S) = 0 \qquad \text{(F–20)}$$

The second to last point in F_2 is calculated using the equations for a first-order filter applied in the reverse direction:

$$F_2(N_S - 1) = \frac{1}{D_{10}}(N_{10}F_1(N_S - 1) + N_{11}F_1(N_S) - D_{11}F_2(N_S))$$

or

$$F_2(N_S - 1) = \frac{1}{D_{10}}(N_{10}F_1(N_S - 1) + N_{11}F_1(N_S)) \qquad \text{(F–21)}$$

Where the coefficients D and N are defined by equation F–16. Note that equations F–20 and F21 must be applied before equation F–18.

Step 3: First Order, Reverse Direction

The first order reverse filter transforms F_2 to the intermediate signal F_3 as follows:

$$F_3(i) = \frac{1}{D_{10}}(N_{10}F_2(i) + N_{11}F_2(i+1) - D_{11}F_3(i+1)) \quad \text{(F–22)}$$

Where F_2 and F_3 are stored as sequential arrays with index values that begin at 1 and increase to N_S along the profile. Equation F–22 is applied by stepping the index value (i) through the range in reverse from $N_S - 1$ to 1. The filter coefficients are defined by equation F–16, above.

The last point in the intermediate signal (F_3) can not be calculated using equation F–22, since it would require values that are out of range of the signal F_2. Instead, F_3 is initialized by assigning the last point in it to zero.

$$F_3(N_S) = 0 \quad \text{(F–23)}$$

Note that equation F–23 must be applied before equation F–22.

Step 4: Second Order, Forward Direction

The second order (complement) filter transforms F_3 to the final signal F_4 as follows:

$$F_4(i) = \frac{1}{D_{20}}(N_{20}F_3(i) + N_{21}F_3(i-1) + N_{22}F_3(i-2) - D_{21}F_4(i-1) - D_{22}F_4(i-2)) \quad \text{(F–24)}$$

Where F_3 and F_4 are stored as sequential arrays with index values that begin at 1 and increase to N_S along the profile. Equation F–24 is applied by stepping the index value (i) through the range from 3 to N_S. The filter coefficients are defined in equation F-19, above.

The first two points in the filtered profile (F_4) can not be calculated using equation F-24, since it would require values that are out of range of the signal F_3. Instead, F_4 is initialized by assigning the first point in it to zero

$$F_4(1) = 0 \quad \text{(F–25)}$$

The second point in F_4 is calculated using the equations for a first-order filter:

$$F_4(2) = \frac{1}{D_{10}}(N_{10}F_3(2) + N_{11}F_3(1) - D_{11}F_4(1))$$

or

$$F_4(2) = \frac{1}{D_{10}}(N_{10}F_3(2) + N_{11}F_3(1)) \quad \text{(F–26)}$$

Where the coefficients D and N are defined by equation F–16. Note that equations F–25 and F–26 must be applied before equation F–24.

References

Karamihas, S. M., "Development of Cross Correlation for Objective Comparison of Profiles." *International Journal of Vehicle Design*, Vol. 36, Nos. 2/3 (2004) pp. 173-193.

Karamihas, S. M., "Critical Profiler Accuracy Requirements." University of Michigan Transportation Research Institute Report UMTRI-2005-24 (2005) 117 p.

La Barre, R. P., et. al., "The Measurement and Analysis of Road Surface Roughness." *Motor Industry Research Association, Report 1970/5* (1970) 31 p.

Perera, R. W. and S. D. Kohn, "Reference Profiler Comparison Mn/ROAD 2006." FHWA contract No. DTFH61-04-D-00010 (2006).

Sayers, M. W., "Dynamic Terrain Inputs to Predict Structural Integrity of Ground Vehicles." *University of Michigan Transportation Research Institute Report UMTRI-88-16* (1988) 114 p.

Sayers, M. W., "On the Calculation of International Roughness Index from Longitudinal Road Profile." *Transportation Research Record 1501* (1995) pp. 1-12.